DOI: 10.1002/ejoc.200800681

Synthetic and Theoretical Investigations on the Construction of Oxanorbornenes by a Michael Addition and Intramolecular Diels–Alder Furan Reaction

Mamta Dadwal,[a] Manoj K. Kesharwani,[b] Vaishalee Danayak,[b] Bishwajit Ganguly,*[b] Shaikh M. Mobin,[c] Rajendran Muruganantham,[a] and Irishi N. N. Namboothiri*[a]

Keywords: Diels–Alder reaction / Michael addition / Oxanorbornene / B3LYP / Ab initio calculations

The conjugate addition of nucleophiles such as allylmercaptan, allyl- and homoallylmalonate and diallylamine to β-furyl enones and acrylate, provides the Michael adducts in good yield. A facile intramolecular Diels–Alder reaction between the unsaturated tether and the furan diene ensues when these adducts are heated in a solvent such as toluene or xylene to afford the cycloadducts in good yield and excellent stereoselectivity in most cases. The structure and stereochemistry of these cycloadducts were confirmed by extensive NMR experiments and X-ray crystallography. Quantum chemical calculations on the transition state and product geometries suggest that the formation of the cycloadducts, in which the newly formed ring is *exo*-fused to the oxanorbornene framework, is favored over the *endo*-fused product due to less strain in the former and its transition state.

Introduction

Intramolecular reactions are superior to their intermolecular counterparts both in terms of substrate reactivity and product selectivity. Whereas the proximal disposition of functional groups that take part in cycloaddition/cyclization provides entropic advantages, the geometric constraints associated with the substrate offer a high degree of regio- and stereoselectivity. Intramolecular Diels–Alder (IMDA) reactions have received great attention, as the two bonds formed simultaneously result in two new rings making it an excellent strategy for the synthesis of polycycles including natural products.[1,2] Although various diene components have been employed in IMDA reactions, the furan diene has figured prominently in the literature because of its reactivity and the cleavage options available for the product oxanorbornene.[3,4] However, the requirement of multi-step reactions to obtain suitable precursors is a major impediment to this otherwise attractive synthetic strategy.

Considerable effort has also been made by using computational methods toward accurate predictions of the stereochemical outcome of many IMDA reactions.[5] Theoretical approaches, including simple FMO models and quantum chemical calculations of transition states and possible intermediates of these reactions, have been considered to explain the regio- and stereoselective aspects of the reaction.[5] In some cases, secondary orbital interactions have been invoked to explain the stereoselectivity observed.[6] Recently, the pseudo-intramolecular Diels–Alder reaction between a 2-substituted furan and an *N*-maleimide has been analyzed with a DFT method.[7]

Recently, we reported a strategy involving the Michael addition and intramolecular Diels–Alder reaction of the furan diene (IMDAF) for the synthesis of oxanorbornenes fused to five- and six-membered rings with conjugated nitroalkenes as the key Michael acceptors.[8] The Michael adducts arising from the addition of various C- and heteroatom-centered nucleophiles to nitroalkenes underwent facile IMDAF reactions in a highly regio- and stereoselective fashion to afford the products in moderate to high yield. Herein, we show the development of this strategy as a full-fledged Michael addition/IMDAF reaction by employing other easily available Michael acceptors such as enones, enediones and acrylates. The products, possessing four contiguous chiral centers, are immediate precursors to fused and functionalized β,γ-enones and cyclohexenols.[8] We also report our theoretical results on the various modes of cycloaddition of the Michael adducts, which show that ring strain can determine the stereoselectivity observed for the IMDA reactions.

[a] Department of Chemistry, Indian Institute of Technology, Bombay, Mumbai 400076, India
[b] Central Salt & Marine Chemicals Research Institute (CSIR), Bhavnagar, Gujarat 364002, India
E-mail: ganguly@csmcri.org
[c] National Single Crystal X-ray Diffraction Facility, Indian Institute of Technology, Bombay, Mumbai 400076, India
Fax: +91-22-2576-7152
E-mail: irishi@iitb.ac.in
Supporting information for this article is available on the WWW under http://www.eurjoc.org or from the author.

Results and Discussion

Initially, we set out to construct a tetrahydrothiophene ring fused to an oxanorbornene framework by the Michael addition/IMDAF strategy. The requisite Michael acceptors, 2-furyl enones **1a**–**c**, were prepared according to reported aldol condensation methods.[9] These Michael acceptors were then treated with allylmercaptan (**2**) in the presence of a suitable base to afford Michael adducts **3** (Table 1). For instance, the triethylamine-mediated addition of allylmercaptan (**2**) to enone **1a** provided Michael adduct **3a** in 64% yield (Table 1, Entry 1). When **3a** was heated in toluene at reflux for 4 d, an IMDAF reaction took place to afford adducts **4a** and **5a** in 67% total yield and an 86:14 ratio. We note that in both the isomers, the tetrahydrothiophene ring was *exo*-fused to the oxanorbornene framework. These isomers are epimeric at the chiral center attached to the S atom.

In a similar fashion, enone **1b** was subjected to the conjugate addition of allylmercaptan (**2**) to afford 1,4-adduct **3b** in comparable yield (63%, Table 1, Entry 2). Subsequently, **3b** was transformed into the IMDAF adducts **4b** and **5b** in 59% yield and an 87:13 ratio. Despite the fact that the IMDAF reaction time was shorter (3 d), similar reaction conditions were suitable for Michael acceptor **1c** possessing two activating (COMe) groups to deliver Michael adduct **3c**, and later, the IMDAF products **4c** and **5c**, in good yield and excellent diastereoselectivity (Table 1, Entry 3).

Encouraged by the simplicity and efficiency of our method in constructing the tricyclic skeleton possessing a fused and functionalized tetrahydrothiophene ring in a stereoselective manner, we felt that the enones **1a**,**b** and acrylate **1d**,[10] containing the key furyl moiety at the β-position, would be suitable for constructing other carbo- and heterocycles fused to oxanorbornenes. We chose allylmalonate **6a** and its homoallyl analog **6b** as the Michael donors for the synthesis of precursors suitable for the IMDAF reaction (Table 2). Allyl and homoallyl Grignard reagents were not suitable for this purpose, as the olefinic moiety in the corresponding Michael adducts would not be sufficiently activated to undergo the IMDAF reaction. The conjugate addition of diethyl allylmalonate (**6a**) to enone **1a** was carried out under solvent-free conditions mediated by KOH and benzyltriethylammonium chloride (TEBAC, Table 2, Entry 1). Michael adduct **7a**, isolated in excellent yield (82%), underwent a smooth IMDAF reaction when heated in toluene for 1 d to afford cycloadducts **8a** and **9a** containing a cyclopentane skeleton in 73% yield and 83:17 selectivity. We also observed a similar high yield and selectivity when enone **1b** was employed as the Michael acceptor

Table 1. Michael addition of allylmercaptan (**2**) to β-furyl enones **1a**–**c** followed by the IMDAF reaction of the Michael adducts **3a**–**c**.

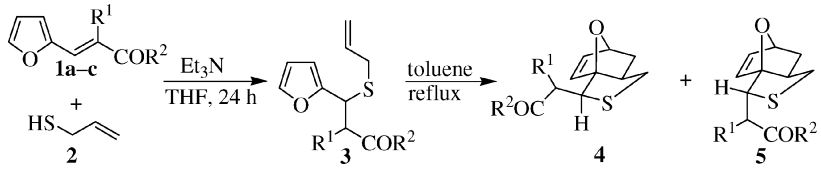

Entry	**1**	R^1, R^2	Yield[a] of **3**	IMDAF time	Yield[a] of **4** + **5**	**4/5**
1	**a**	H, Me	64%	4 d	67%	86:14
2	**b**	H, Ph	63%	4 d	59%	87:13
3	**c**	COMe, Me	59%	3 d	51%	87:13[b]

[a] Isolated yield after purification by silica gel column chromatography. [b] The minor isomer **5c** could not be isolated in pure form.

Table 2. Michael addition of allyl- and homoallylmalonates **6**[a] to β-furyl enones **1a**,**b** and acrylate **1d** followed by an IMDAF reaction of the Michael adducts **7**.

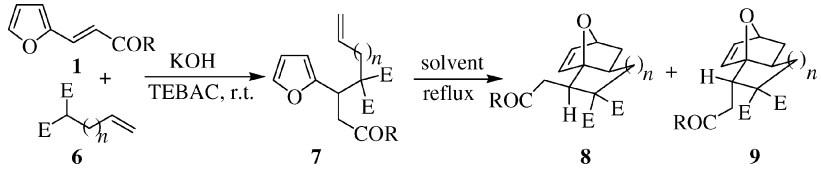

Entry	**1**	R	**6**, *n*	MA time	Product, yield[b]	IMDAF solvent and time	Yield[b] of **8** + **9**	**8/9**
1	**a**	Me	**6a**, 1	10 h	**7a**, 82%	toluene, 1 d	73%	83:17
2	**b**	Ph	**6a**, 1	8 h	**7b**, 77%	toluene, 1 d	87%	82:18
3	**d**	OEt	**6a**, 1	72 h	**7c**, 38%	toluene, 1.5 d	77%	84:16
4	**a**	Me	**6b**, 2	16 h	**7d**, 75%	xylene, 7 d	41%[c]	100:0
5	**b**	Ph	**6b**, 2	15 h	**7e**, 69%	xylene, 5 d	43%[d]	93:7
6	**d**	OEt	**6b**, 2	106 h	**7f**, 45%	xylene, 7 d	–[e]	–

[a] **6**: E = CO_2Et. [b] Isolated yield after purification by silica gel column chromatography. [c] 40% of Michael adduct **7d** was recovered. [d] 35% of Michael adduct **7e** was recovered. [e] 38% of **7f** plus intractable material was recovered.

(Table 2, Entry 2). Although the yield of Michael adduct **7c** was low (38%) when acrylate **1d** was treated with allylmalonate **6a**, **7c** subsequently underwent an IMDAF reaction to provide **8c** and **9c** in high yield (77%) and selectivity (84:16, Table 2, Entry 3).

We subsequently used substrates **1a**,**b** and **1d** to construct a cyclohexane skeleton fused to oxanorbornene (Table 2, Entries 4–6). Thus, whereas the 1,4-addition of homoallylmalonate **6b** to enones **1a**,**b** proceeded well (75 and 69% yield, respectively, Table 2, Entries 4 and 5), the corresponding reaction of **6b** with acrylate **1d** provided adduct **7f** only in moderate yield (45%, Table 2, Entry 6). Nevertheless, we subjected these Michael adducts to the IMDAF reaction by refluxing them in xylene for 5–7 d (Table 2, Entries 4–6). As anticipated, these reactions remained incomplete even after such a prolonged reaction time, and considerable amounts of Michael adducts were recovered. However, the selectivities in these reactions were noteworthy. Whereas we observed 100% selectivity when **7d** was subjected to the IMDAF reaction (Table 2, Entry 4), the reaction of **7e** also exhibited excellent selectivity (Table 2, Entry 5).

Having constructed the tetrahydrothiophene, cyclopentane and cyclohexane rings, we investigated the synthesis of a pyrrolidine ring by our Michael/IMDAF strategy. Unfortunately, our attempted Michael addition of diallylamine (**10**) to enones **1a**,**b** under a variety of conditions provided either no product or a complex mixture. However, we succeeded in adding diallylamine (**10**) to (2-furyl)acrylate **1d** under *n*-butyllithium-mediated conditions in 79% yield (Table 3, Entry 1). Michael adduct **11d** underwent a facile IMDAF reaction when refluxed in toluene for 2 d to afford adducts **12d** and **13d** in a combined yield of 89% and a 23:77 ratio. Analogously, furylidenemalonate **1e**[11] provided Michael adduct **11e**, which was refluxed without purification in toluene for 4 d to obtain pyrrolidines **12e** and **13e** in lower yield (73%), but better selectivity (18:82, Table 3, Entry 2). We note that in contrast to the predominance of *exo-cis* isomers **4** and **8** over *exo-trans* isomers **5** and **9** in the case of tetrahydrothiophenes **4**,**5** (Table 1) and cyclopentanes **8**,**9** (Table 2), respectively, we obtained *exo-trans* isomers **13** as the major products in the case of pyrrolidines **12**,**13** (Table 3, and see also the discussion of the NMR and computational results below).

All our attempts to add allyl alcohol to enones and acrylates under a variety of conditions met with failure. Therefore, we could not generate a tetrahydrofuran ring by our Michael/IMDAF strategy. In another attempt to synthesize a seven-membered ring fused to oxanorbornene, we carried out the Michael addition of diallyl malonate (**14**) to 4-(2-furyl)but-3-en-2-one (**1a**), but the subsequent cycloaddition of Michael adduct **15** to the desired IMDAF adduct **16** did not proceed, even under forcing conditions (refluxing xylene or mesitylene, Scheme 1).

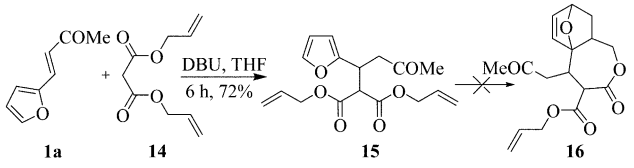

Scheme 1.

Structure and Stereochemistry

If we consider the two modes of the IMDAF reaction, eight cycloadducts (**18**–**25**) are theoretically possible; four cycloadducts (**18**–**21**) would result from C2–C4′ and C5–C5′ bonding (path A), and the other four (**22**–**25**) would derive from C2–C5′ and C5–C4′ bonding (path B, Scheme 2). Whereas path A provides fused or "*ortho*" products, path B leads to bridged or "*meta*" products. However, path B appeared geometrically unfavorable as shown in Figure 1. In this path, severe strain is expected if the reacting centers in the Michael adduct that are relatively far apart have to come closer together. Therefore, we excluded path B and the associated cycloadducts **22**–**25** from further analysis.

We carried out extensive NMR studies to establish the structure and stereochemistry of the cycloadducts. At the outset, we chose the isomers **4b/5b** as representative examples, and we correctly assigned the protons with the assistance of a ^{1}H-^{1}H COSY experiment. Further analysis of the

Table 3. Michael addition of diallylamine (**10**)[a] to β-furylacrylate **1d** and furylidenemalonate **1e** followed by an IMDAF reaction of Michael adducts **11**.

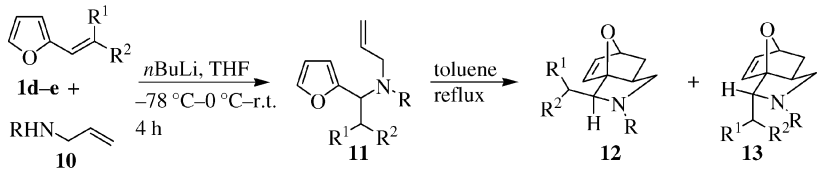

Entry	1	R^1, R^2	Product, yield[b]	IMDAF time	Yield[b] of 12 + 13	12/13
1	**d**	H, CO_2Et	**11d**, 79%	2 d	89%	23:77
2	**e**	CO_2Et, CO_2Et	**11e**, –[c]	4 d	73%	18:82

[a] **10**: R = allyl. [b] Isolated yield after purification by silica gel column chromatography. [c] Crude Michael adduct **11e** was used for the next (IMDAF) step.

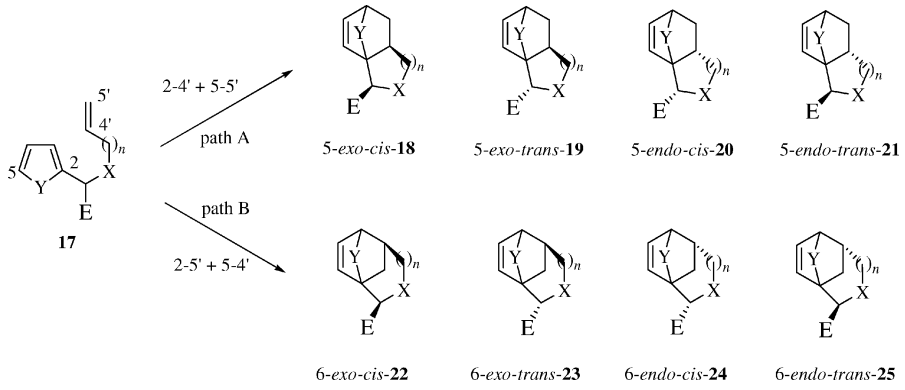

Scheme 2.

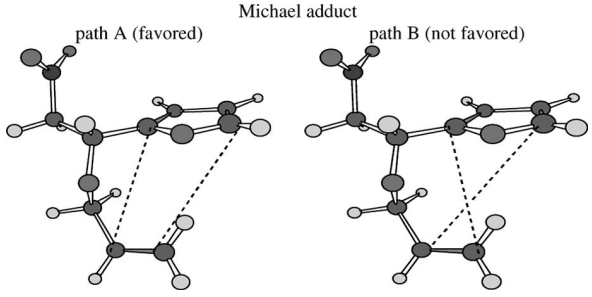

Figure 1. Two modes of cycloaddition of the Michael adduct.

^{1}H-^{1}H couplings in **4b** and **5b** suggested that the newly formed ring was *exo*-fused to the oxanorbornene moiety, as in the previously reported cycloadducts obtained from the Michael-initiated IMDAF reaction of nitro compounds.[8] We observed in **4b** and **5b** that out of the two geminal protons H-7α and H-7β, only H-7β coupled with H-6 (J = 4.4 and 4.5 Hz, respectively, in **4b** and **5b**, Table 4, Entries 1 and 2). We observed no coupling between H-6 and H-7α due to a dihedral angle of ca. 90° between the two protons. Whereas the coupling for H-7α with H-7a was moderately strong (J = 7.3 and 7.7 Hz, respectively, in **4b** and **5b**), that between H-7β and H-7a was weak (J = 2.6 Hz in both **4b** and **5b**, Table 4, Entries 4 and 5). Subsequently, we analyzed the 2D-NOESY data for the two isomers, which showed a medium (in **4b**) and weak (in **5b**) NOE between H-6 and H-7β (Table 4, Entry 2), but no NOE (in **4b**) or a weak NOE (in **5b**) between H-6 and H-7α (Table 4, Entry 1). We observed no NOE between H-7β and H-7a for either **4b** or **5b** (Table 4, Entry 5).

After establishing that the newly formed ring was *exo*-fused to the oxanorbornene framework, we addressed the stereochemistry at position 3. The analysis of the ^{1}H and ^{1}H-^{1}H COSY NMR spectra did not divulge much information due to (i) the small difference in the coupling of H-3 with the H-9 and H-9′ protons (Table 4, Entries 9 and 10) and (ii) the absence of any other couplings for H-3. However, weak and medium NOEs for H-4 with H-9 and H-9′, respectively, in **5b** suggested that the benzoyl group was α-oriented in **5b** (Table 4, Entries 12 and 13). This was further supported by the absence of any NOE for H-4 with H-9 or H-9′ in **4b**, which was indicative of the β-orientation of the benzoyl group in **4b** (Table 4, Entries 12 and 13). These results agreed well with those obtained for corresponding nitro compounds.[8] Finally, we unambiguously established the structure and stereochemistry by single-crystal X-ray analysis of analog **8b** (Figure 2). For instance, a dihedral angle of 168.6° for C1–C7a–C3a–C4 in **8b** confirmed that the five-membered ring was *exo*-fused to the oxanorbornene, and a dihedral angle of 24.6° for O8–C3a–C3–C9 confirmed the pseudo-equatorial orientation of the substituent at C-3 (numbering as in **4b**,**5b**, Table 4).

Unlike in the case of tetrahydrothiophenes **4**,**5** and cyclopentanes **8**,**9**, we could not independently analyze the stereochemistry at C-3 in pyrrolidines **12**,**13** (see Table 3) by 2D-NMR experiments or X-ray crystallography. Whereas the 2D-NOESY spectra of **12d**,**e** and **13d**,**e** showed no characteristic NOEs, all these samples were liquids, and attempts to prepare solid derivatives suitable for single-crystal X-ray analysis were unsuccessful. Finally, a careful analysis of the ^{1}H NMR chemical shifts of H-3 in *exo-cis*

Table 4. Comparison of ^{1}H NMR, ^{1}H-^{1}H 2D-COSY and ^{1}H-^{1}H 2D-NOESY characteristics of isomers **4b** and **5b**.

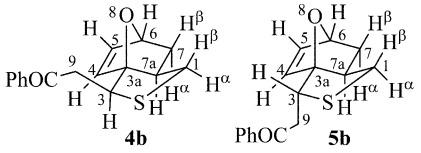

Entry	^{1}H-^{1}H	4b		5b	
		J [Hz]	NOE[a]	J [Hz]	NOE[a]
1	6-7α	0.0	–	0.0	W
2	6-7β	4.4	M	4.5	W
3	7α-7β	11.7	S	11.7	S
4	7α-7a	7.3	M	7.7	S
5	7β-7a	2.6	–	2.6	–
6	7a-1α	7.7	M	10.6	–
7	7a-1β	10.6	M	10.5	–
8	1α-1β	10.6	S	10.9	S
9	3-9	18.3	W	17.2	M
10	3-9′	8.8	W	9.2	M
11	3-4	–	–	–	–
12	4-9	–	–	–	W
13	4-9′	–	–	–	M

[a] S = Strong; M = Medium; W = Weak.

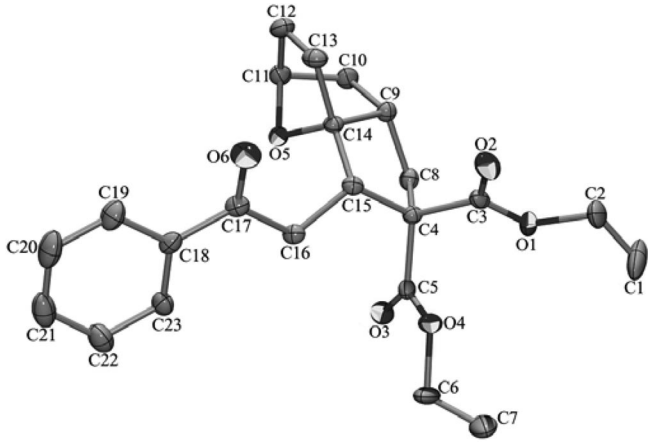

Figure 2. Single-crystal X-ray structure of **8b**.

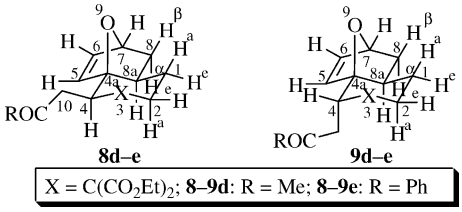

Figure 3. Stereochemistry of **8d**,**e** and **9d**,**e**.

isomers **4** and **8** and *exo-trans* isomers **5** and **9** suggested that H-3 is considerably deshielded in *exo-cis* isomers as compared to *exo-trans* isomers (Table 5, Entries 1–6). We extended this key feature to the stereochemical analysis of **12d**,**e** and **13d**,**e**. Thus, since H-3 was deshielded in the minor products **12d**,**e** (Table 5, Entries 7 and 8), we assigned the *exo-cis* stereochemistry to **12d**,**e**. We further corroborated this assignment with results from high-level quantum chemical calculations (vide infra), which predicted the preference for *exo-trans* isomer **13** over *exo-cis* isomer **12** in the case of pyrrolidines **12**,**13**.

Table 5. Comparison of the ^{1}H NMR chemical shifts of H-3 in tetrahydrothiphenes **4**,**5**, cyclopentanes **8**,**9** and pyrrolidines **12**,**13**.

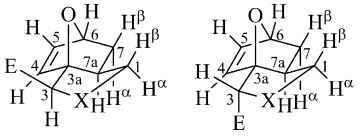

exo-cis- **-4**, **-8**, **-12** *exo-trans-* **-5**, **-9**, **-13**

Entry	X	E	δ of H-3 signal [ppm] *exo-cis-*	*exo-trans-*
1	S	CH_2COCH_3	**4a**: 4.22	**5a**: 3.97
2	S	CH_2COPh	**4b**: 4.45	**5b**: 4.20
3	S	$CH(COCH_3)_2$	**4c**: 4.50	**5c**: –
4	$C(CO_2Et)_2$	CH_2COCH_3	**8a**: 3.90	**9a**: 3.45
5	$C(CO_2Et)_2$	CH_2COPh	**8b**: 4.00	**9b**: 3.47–3.67
6	$C(CO_2Et)_2$	CH_2CO_2Et	**8c**: 3.90	**9c**: 3.43
7	N-allyl	CH_2CO_2Et	**12d**: 3.64	**13d**: 3.27–3.30
8	N-allyl	$CH(CO_2Et)_2$	**12e**: 3.64	**13e**: 3.22–3.29

The structural and stereochemical assignment of **8d**, **8e** and **9e** were complicated by the overlapping peaks in their ^{1}H NMR spectra. For instance, since the H-1a, H-1e, H-2a, H-2e, H-8α, H-8β protons (Figure 3) appeared in the narrow range of δ = 1.30–1.90 ppm, we could not independently assign the stereochemistry of ring fusion between the oxanorbornene framework and the six-membered ring. The absence of any appreciable scalar coupling or NOE interaction for H-4 with protons other than H-10 and H-10′ also made the stereochemical assignment at C-4 extremely difficult. Therefore, we unambiguously established the structure and stereochemistry of one representative compound (**8e**) by single-crystal X-ray analysis (Figure 4). Whereas a dihedral angle of 174.5° for C5–C4a–C8a–C1 confirmed that the six-membered ring is *exo*-fused to the oxanorbornene, a dihedral angle of 61.4° for O9–C4a–C4–C10 confirmed the equatorial orientation of the substituent at C-4 in **8e**.

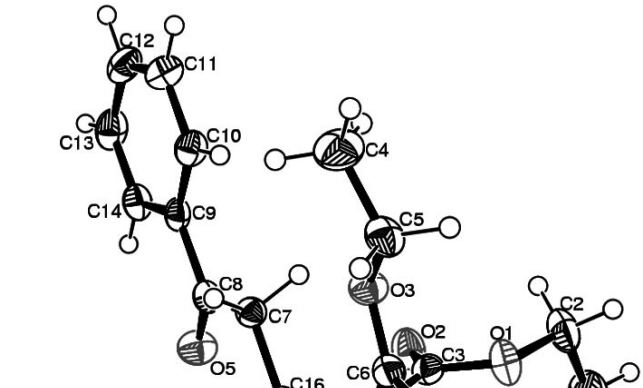

Figure 4. Single-crystal X-ray structure of **8e**.

Computational Results

In order to probe the selectivities observed during the intramolecular cycloadditions, we examined computationally the formation of all the cycloadducts **18**–**21** by path A (Figure 1 and Scheme 3) for X = S, N-allyl and $C(CO_2Me)_2$.[12,13] We performed the calculations with E = CH_2CHO in this study for simplicity. We calculated the relative energies of the four possible reaction products (**18**–**21**) and their transition states at the RHF/3-21G*[14] and B3LYP/6-31G*//RHF/3-21G*[15] levels of theory (Scheme 3). The calculated results, summarized in Table 6, clearly show that *exo* isomers **18**,**19** were preferred over *endo* isomers **20**,**21** in all cases. The relative energies of products **18**–**21** predict the formation of *exo-cis* isomers **18** for X = S and $C(CO_2Me)_2$ at both levels of theory (Table 6, Entries 1–3, 8 and 9). In order to examine the effect of dif-

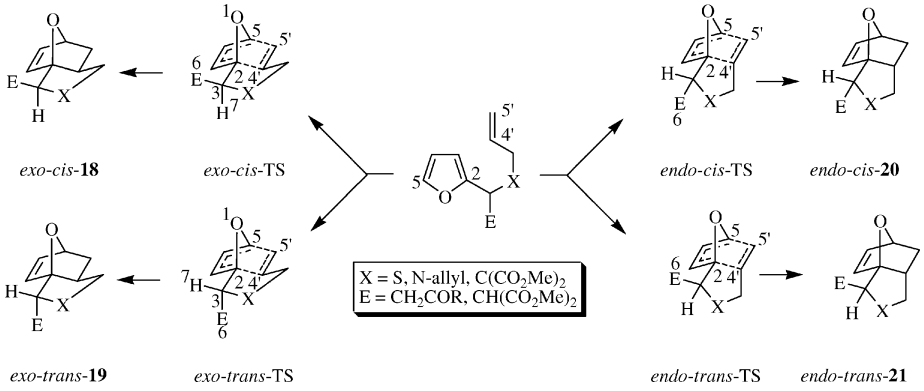

Scheme 3.

Table 6. RHF/3-21G*- and B3LYP/6-31G*//RHF/3-21G*-calculated relative energies of the products **18**–**21** and their transition states in kcal mol^{-1}.

Entry	X	E	Theory level	Product				Transition state			
				exo-cis-**18**	*exo-trans*-**19**	*endo-cis*-**20**	*endo-trans*-**21**	*exo-cis*	*exo-trans*	*endo-cis*	*endo-trans*
1	S	CH_2CHO	RHF[a]	0.0	5.6	15.4	11.4	0.0	3.0	10.6	7.7
2			B/R[b]	0.0	2.9	11.5	8.6	0.0	0.9	8.9	6.4
3			B3[c]	0.0	3.0	12.1	8.5	0.0	1.1	9.7	6.7
4	N-allyl	CH_2CHO	RHF	0.0	0.8	14.0	13.7	2.8	0.0	12.9	7.3
5			B/R	1.3	0.0	13.5	14.6	5.1	0.0	11.5	8.4
6		CHZ_2[d]	RHF	3.3	0.0	19.3	16.4	3.8	0.0	16.4	11.4
7			B/R	4.6	0.0	18.1	16.1	6.5	0.0	16.0	13.3
8	CZ_2[d]	CH_2CHO	RHF	0.0	2.3	11.0	12.3	0.0	1.0	7.0	9.5
9			B/R	0.0	1.3	9.9	10.9	1.6	0.0	8.9	9.7

[a] Relative energies at the RHF/3-21G* level. [b] Relative energies at the B3LYP/6-31G* level. [c] B3LYP/6-31+G*-optimized relative energies. [d] Z = CO_2Me.

fuse functions, when a heteroatom such as S is present in the system, we performed calculations at the B3LYP/6-31+G* level for X = S (Table 6, Entry 3). The calculated relative energy differences for transition state and ground state geometries were similar to results obtained at the RHF/3-21G* and B3LYP/6-31G**//RHF/3-21G* levels. Since the larger and smaller basis sets gave similar results, this justified the general use of the smaller basis set.

Unlike in the case of X = S and $C(CO_2Me)_2$, where the *exo-cis* isomer **18** was predicted and experimentally observed as the major product (Table 6, Entries 1–3, 8 and 9), our calculations favored the *exo-trans* isomer **19** for X = N-allyl at the B3LYP/6-31G* level (Table 6, Entry 5). To examine the discrepancy between the results for **19** from the two methods, we performed additional calculations with E = $CH(CO_2Me)_2$ (Table 6, Entries 6 and 7). The calculated results show that the *exo-trans* configuration was preferred over the *exo-cis* configuration at both levels of theory. Extending the study to transition state energy calculations, the results show that the formation of *exo-cis* isomers **18** was favored when X = S and $C(CO_2Me)_2$ (Table 6, Entries 1–3, 8 and 9), whereas the *exo-trans* isomer **19** was favored for X = N-allyl (Table 6, Entry 4–7). However, the B3LYP/6-31G*//RHF/3-21G* result for X = $C(CO_2Me)_2$ showed the preferential formation of the *exo-trans* transition state. The formation of the major *exo-cis* isomers for X = S, $C(CO_2Me)_2$ and *exo-trans* for N-allyl agreed well with the experimentally observed products (Tables 1, 2, and 3). The reaction energies calculated for these IMDAF reactions were exergonic for the *exo* products; however, *endo* products were generally endergonic (Table 7). The transition state geometries for the *exo* and *endo* isomers indicated a concerted reaction mechanism; however, the extent of bond formation was slightly asymmetrical (Table S1).

Table 7. RHF/3-21G*- and B3LYP/6-31G*//RHF/3-21G*-calculated reaction energies of various IMDAF reactions in kcal mol^{-1}.

Entry	X	E	Theory level	Reaction energy			
				exo-cis	*exo-trans*	*endo-cis*	*endo-trans*
1	S	CH_2CHO	RHF[a]	–16.5	–10.9	–1.2	–5.1
2			B/R[b]	–3.4	–0.5	+8.2	+5.2
3	N-allyl	CH_2CHO	RHF	–12.2	–11.4	+1.8	+1.5
4			B/R	–2.2	–3.5	+10.0	+11.1
5		CHZ_2[c]	RHF	–13.2	–16.5	+2.8	–0.1
6			B/R	–0.8	–5.4	+12.7	+8.8
7	CZ_2[c]	CH_2CHO	RHF	–15.6	–13.3	–4.6	–3.3
8			B/R	–4.4	–3.2	+5.5	+6.5

[a] Reaction energies at the RHF/3-21G* level. [b] Reaction energies at the B3LYP/6-31G* level. [c] Z = CO_2Me.

The activation energies are higher for these IMDAF reactions. For the preferred *exo-cis* isomer (X = S), the activation energy calculated at the B3LYP/6-31+G* level was 28.9 kcal mol^{-1}. The incorporation of activation entropy at 110 °C enhanced the activation free energy to 34.4 kcal mol^{-1}. These results suggest that the negative activation entropy (–14.3 eu) was much lower in this case,

which led to the formation of the 7-oxanorbornene ring. In comparison, for the intermolecular DA reaction of butadiene and ethylene, the calculated activation entropy was –40.6 eu, and the activation free energy at the experimental temperature of 165 °C was 42.6 kcal mol^{-1}.[7] The large activation free energy for butadiene and ethylene is due to the large activation entropy associated with this reaction.

The calculated results suggest that the formation of *exo* isomers was both thermodynamically and kinetically preferred over that of the *endo* isomers. Therefore, even if there was a retro-Diels–Alder reaction, one can envisage that the products formed would be as predicted and observed. The formation of the *exo* isomer as the major product from the IMDAF reaction appeared to result from the difference in strain induced in the ring systems. To examine this, we took the stable *exo-cis*-**18** and *endo-trans*-**21** isomers for X = S as model systems (Table 6, Entry 1). The 7-oxanorbornene rings formed in these isomers were isolated from the calculated geometries. Substituents were replaced by hydrogen atoms without perturbing the geometry of the 7-oxanorbornane rings (Figure 5). The energies calculated for the 7-oxanorbornene rings derived from the X = S product, and transition state geometries suggest that the newly formed norbornene ring in the *exo* isomer was much more stable than that in the *endo* form at both the RHF/3-21G* and B3LYP/6-31+G* levels of theory (Table 8). It appears that ring strain contributed predominantly towards the formation of the *exo* isomers in these cases.

Figure 5. 7-Oxanorbornene ring.

Table 8. RHF/3-21G*- and B3LYP/6-31+G*-calculated energy differences [kcal mol^{-1}] for 7-oxanorbornene rings derived from **18** and **21** (X = S) and transition state geometries.

Entry	Configuration	Theory level	Product	Transition state
1	*exo-cis*	RHF[a]	0.0	0.0
2		B/R[b]	0.0	0.0
3	*endo-trans*	RHF	6.6	4.3
4		B/R	5.9	3.9

[a] Relative energies at the RHF/3-21G* level. [b] Relative energies at the B3LYP/6-31+G* level.

Further, we found the subtle difference in the stereochemistry of the products with X = S, CO_2Me versus those with X = N-allyl interesting. Whereas the Michael adducts with X = S and CO_2Me provided *exo-cis* isomers, those with X = N-allyl gave *exo-trans* isomers. The difference in the stereochemistry presumably arose from the torsional effect in these systems.[16] Examining the torsion angles in the ground state geometries of the *exo-cis* isomer (τ_1 = O1–C2–C3–C6) and of the *exo-trans* isomer (τ_2 = O1–C2–C3–H7) for X = S and N-allyl suggested that τ_1 (29.5°) was more staggered than τ_2 (17.6°) in the case of X = S (Figure 6). However, the values were reversed for X = N-allyl, as τ_1 = 29.4° and τ_2 = 32.4°, respectively (Figure 6).

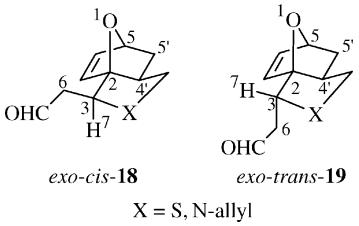

Figure 6. *exo* products for X = S and N-allyl.

Conclusions

The synthesis of oxanorbornenes fused to five- and six-membered carbocycles and heterocycles was carried out in good yield and high stereoselectivity from readily available β-furyl enones, an enedione and an acrylate. The protocol involved the Michael addition of nucleophiles possessing an unsaturated tether to the β-furyl α,β-unsaturated carbonyl compounds followed by an intramolecular Diels–Alder reaction between the furan diene and the olefinic moiety. We rationalized the high stereoselectivity observed in these cycloadditions through quantum chemical calculations. These calculations revealed that the *exo*-fused cycloadduct was kinetically and thermodynamically favored over its *endo*-fused isomer due to the difference in the strain for the formation of 7-oxanorbornene rings in the transition states and products. The dependence of the *cis* or *trans* stereochemistry upon different substituents in the isomers arose from a torsional effect.

Experimental Section

General: Melting points were recorded with a Thermonik melting point apparatus and are uncorrected. IR spectra were recorded with an Impact 400/Nicolet or Perkin–Elmer Spectrum One FT spectrometer. NMR spectra (^{1}H, ^{13}C, ^{1}H-^{1}H COSY and ^{1}H-^{1}H NOESY) were recorded with TMS as the internal standard with an AMX-400 (Varian Mercury Plus OXFORD, broad band, auto switchable and inverse probe) or VXR-300S spectrometer. The coupling constants (*J* values) are given in Hz. Mass spectra (low and high resolution) were recorded at 60–70 eV with a Micromass Q-TOF mass spectrometer under ESI mode. X-ray data were collected with a Nonius MACH 3 diffractometer equipped with graphite-monochromated Mo-K_α radiation. The structures were solved by direct methods with SHELXS97 and refined by full-matrix least-squares against F^2 with SHELXL97 software. CCDC-693540 (for **8b**) and -693541 (for **8e**) contain the supplementary crystallographic data for this paper. These data can be obtained free of charge from the Cambridge Crystallographic Data Centre via www.ccdc.cam.ac.uk/data_request/cif. Michael acceptors **1a**–**e** were prepared according to literature methods.[9–11]

Computational Methodology: All calculations were performed at the RHF/3-21G* level of theory with the JAGUAR program.[12] Complete vibrational analyses were performed to characterize the transition state and ground state geometries. In addition, single

point B3LYP/6-31G* calculations[13] with RHF/3-21G*-optimized geometries were performed to estimate the energies of the transition states and ground states of these IMDAF reactions. To examine the basis set dependence on the energetics of the transition states and ground states, the *S*-substituted derivative (X = S) was optimized with the 6-31+G* basis set at the B3LYP level.

General Procedure for the Michael Addition of Allylmercaptan (2) to 2-Furyl Enones 1a–c: To a stirred solution of allylmercaptan (**2**, 0.62 mL, 1.1 mmol) in THF (5 mL) at 0 °C under nitrogen was added Et_3N (0.01 mL, 0.1 mmol) followed by a solution of **1a**, **1b** or **1c** (1 mmol) in THF (5 mL). After the addition was complete, the reaction mixture was stirred at reflux for 24 h. The reaction mixture was then diluted with water (5 mL) and acidified with HCl (10%, 10 mL). The aqueous layer was extracted with ethyl acetate (3 × 15 mL). The combined organic layers were then washed with brine (20 mL), dried with anhydrous Na_2SO_4 and concentrated in vacuo. The crude residue was then purified by silica gel chromatography with ethyl acetate/*n*-hexane (1:50 to 1:25) as the eluent to afford pure **3a**, **3b** or **3c**.

4-(Allylthio)-4-(furan-2-yl)butan-2-one (3a): Light yellow oil. Yield 64% (135 mg). IR (neat): $\tilde{\nu}$ = 2917 (w), 1721 (s), 1361 (m), 1151 (m) cm^{-1}. ^1H NMR (300 MHz, $CDCl_3$): δ = 2.15 (s, 3 H), 3.04 (ABqd, J = 17.1, 6.8 Hz, 2 H), 3.01–3.10 (m, 2 H), 4.38 (t, J = 7.3 Hz, 1 H), 5.10–5.17 (m, 2 H), 5.70–5.84 (m, 1 H), 6.17 (d, J = 3.4 Hz, 1 H), 6.30 (dd, J = 3.4, 2.0 Hz, 1 H), 7.35 (d, J = 2.0 Hz, 1 H) ppm. ^{13}C NMR (75 MHz, $CDCl_3$): δ = 30.5, 34.4, 36.1, 47.0, 107.1, 110.3, 117.6, 134.0, 142.1, 153.5, 205.1 ppm. MS (ESI, Ar): *m*/*z* (%) = 233 (100) $[M + Na]^+$. HRMS (ESI, Ar): calcd. for $C_{11}H_{14}O_2NaS$ $[M + Na]^+$ 233.0612; found 233.0619.

3-(Allylthio)-3-(furan-2-yl)-1-phenylpropan-1-one (3b): Light yellow oil. Yield 63% (172 mg). IR (neat): $\tilde{\nu}$ = 2912 (w), 1688 (s), 1448 (w), 1353 (w), 1229 (w) cm^{-1}. ^1H NMR (300 MHz, $CDCl_3$): δ = 3.09–3.13 (unresolved m, 2 H), 3.60 (ABqd, J = 17.2, 6.6 Hz, 2 H), 4.61 (dd, J = 7.7, 6.6 Hz, 1 H), 5.08–5.17 (m, 2 H), 5.70–5.84 (m, 1 H), 6.20 (d, J = 3.3 Hz, 1 H), 6.27 (dd, J = 3.3, 1.8 Hz, 1 H), 7.33 (d, J = 1.8 Hz, 1 H), 7.41–7.95 (m, 5 H) ppm. ^{13}C NMR (75 MHz, $CDCl_3$): δ = 34.4, 36.3, 42.3, 107.0, 110.2, 117.5, 128.1, 128.6, 133.3, 134.0, 136.5, 142.0, 153.7, 196.3 ppm. MS (ESI, Ar): *m*/*z* (%) = 295 (100) $[M + Na]^+$, 105 (12). HRMS (ESI, Ar): calcd. for $C_{16}H_{16}O_2NaS$ $[M + Na]^+$ 295.0769; found 295.0756.

3-[(Allylthio)(furan-2-yl)methyl]pentane-2,4-dione (3c): Light yellow oil. Yield 59% (149 mg). IR (neat): $\tilde{\nu}$ = 3055 (m), 2984 (m), 2922 (m), 1734 (s), 1703 (s), 1423 (m), 1358 (m), 1266 (s), 740 (s) cm^{-1}. ^1H NMR (300 MHz, $CDCl_3$): δ = 2.03 (s, 3 H, keto form), 2.17 (s, 6 H, enol form), 2.31 (s, 3 H, keto form), 2.98–3.14 (m, 2 H, keto form), 3.20–3.30 (m, 2 H, enol form), 4.47 (ABq, J = 12.0 Hz, 2 H, keto form), 4.93 (s, 1 H, enol form), 5.08–5.22 (m, 2 H, keto and enol forms), 5.66–5.82 (m, 1 H, keto form), 5.83–5.96 (m, 1 H, enol form), 6.18 (d, J = 3.7 Hz, 1 H, keto form), 6.27–6.29 (m, 1 H, enol form), 6.30 (dd, J = 3.7, 2.0 Hz, 1 H, keto form), 6.34 (dd, J = 3.7, 2.0 Hz, 1 H, enol form), 7.35–7.36 (m, 1 H, keto and enol forms), 17.28 (br. s, 1 H, enol form) ppm. ^{13}C NMR (100 MHz, $CDCl_3$): δ = 29.3 (q, keto form), 34.2 (t, keto form), 39.9 (d, keto form), 71.4 (d, keto form), 108.2 (d, keto form), 110.4 (d, keto form), 118.1 (t, keto form), 133.3 (d, keto form), 142.4 (d, keto form), 151.3 (s, keto form), 200.7 (s, keto form), 29.2 (q, enol form), 35.3 (t, enol form), 38.8 (d, enol form), 107.6 (d, enol form), 110.1 (s, enol form), 110.5 (d, enol form), 118.0 (t, enol form), 134.0 (d, enol form), 142.1 (d, enol form), 153.7 (s, enol form), 200.9 (s, enol form) ppm. MS (ESI, Ar): *m*/*z* (%) = 275 (55) $[M + Na]^+$, 227 (100), 153 (15). HRMS (ESI, Ar): calcd. for $C_{13}H_{16}O_3NaS$ $[M + Na]^+$ 275.0718; found 275.0709.

General Procedure for the Michael Addition of Diethyl Allylmalonate (6a) and Diethyl Homoallylmalonate (6b) to Enones 1a,b and Acrylate 1d: To a stirred mixture of **1a**, **1b** or **1d** (1 mmol) and diethyl allylmalonate (**6a**, 600 mg, 3 mmol) or diethyl homoallylmalonate (**6b**, 642 mg, 3 mmol) was added benzyltriethylammonium chloride (TEBAC, 14 mg, 0.06 mmol) followed by powdered KOH (3.3 mg, 0.06 mmol). The mixture was stirred until the reaction was complete (as monitored by TLC, see also Table 2) and filtered. The filtrate was concentrated in vacuo. The crude mixture was then purified by silica gel chromatography with ethyl acetate/*n*-hexane (1:10 to 1:5) as the eluent to afford pure **7a**–**f**.

Diethyl 2-Allyl-2-[1-(furan-2-yl)-3-oxobutyl]malonate (7a): Light yellow oil. Yield 82% (275 mg). IR (neat): $\tilde{\nu}$ = 3055 (w), 2985 (m), 1724 (s), 1266 (s) cm^{-1}. ^1H NMR (400 MHz, $CDCl_3$): δ = 1.24 (t, J = 7.3 Hz, 3 H), 1.29 (t, J = 7.3 Hz, 3 H), 2.06 (s, 3 H), 2.53 (ABqd, J = 14.7, 7.3 Hz, 2 H), 3.00 (dd, J = 17.4, 2.8 Hz, 1 H), 3.14 (dd, J = 17.4, 10.5 Hz, 1 H), 4.08 (dd, J = 10.5, 2.8 Hz, 1 H), 4.11–4.27 (m, 4 H), 5.05–5.09 (m, 2 H), 5.71–5.82 (m, 1 H), 6.12 (d, J = 2.9 Hz, 1 H), 6.25 (dd, J = 2.9, 1.8 Hz, 1 H), 7.27 (d, J = 1.8 Hz, 1 H) ppm. ^{13}C NMR (100 MHz, $CDCl_3$): δ = 13.7, 13.8, 29.7, 37.4, 38.2, 44.4, 60.4, 61.1 (2 C), 108.3, 110.0, 118.7, 132.5, 141.4, 152.4, 169.5, 169.8, 205.6 ppm. MS (ESI, Ar): *m*/*z* (%) = 359 (100) $[M + Na]^+$. HRMS (ESI, Ar): calcd. for $C_{18}H_{24}O_6Na$ $[M + Na]^+$ 359.1471; found 359.1475.

Diethyl 2-Allyl-2-[1-(furan-2-yl)-3-oxo-3-phenylpropyl]malonate (7b): Colorless oil. Yield 77% (307 mg). IR (neat): $\tilde{\nu}$ = 3058 (w), 2984 (w), 1728 (s), 1688 (m), 1266 (s) cm^{-1}. ^1H NMR (300 MHz, $CDCl_3$): δ = 1.23 (t, J = 7.0 Hz, 3 H), 1.33 (t, J = 7.0 Hz, 3 H), 2.59 (ABqd, J = 14.4, 7.2 Hz, 2 H), 3.53 (dd, J = 17.6, 2.3 Hz, 1 H), 3.78 (dd, J = 17.6, 10.5 Hz, 1 H), 4.14–4.20 (m, 1 H), 4.22–4.38 (m, 4 H), 5.11 (m, 2 H), 5.81 (m, 1 H), 6.14 (d, J = 3.0 Hz, 1 H), 6.22 (dd, J = 3.0, 1.4 Hz, 1 H), 7.25 (d, J = 1.4 Hz, 1 H). 7.40–7.60 (m, 3 H), 7.92–7.94 (m, 2 H) ppm. ^{13}C NMR (75 MHz, $CDCl_3$): δ = 14.2 (2 C), 38.0, 38.7, 40.1, 61.0, 61.5 (2 C), 108.7, 110.2, 119.0, 128.1, 128.6, 133.0 (×2), 136.9, 141.7, 152.7, 170.1, 170.2, 197.5 ppm. MS (ESI, Ar): *m*/*z* (%) = 421 (72) $[M + Na]^+$, 199 (62). HRMS (ESI, Ar): calcd. for $C_{23}H_{26}O_6Na$ $[M + Na]^+$ 421.1627; found 421.1622.

Triethyl 2-(Furan-2-yl)hex-5-ene-1,3,3-tricarboxylate (7c): Light yellow oil. Yield 38% (139 mg). IR (neat): $\tilde{\nu}$ = 3079 (m), 2984 (s), 2939 (s), 2907 (m), 1729 (br., s), 1445 (s), 1266 (s) cm^{-1}. ^1H NMR (300 MHz, $CDCl_3$): δ = 1.15 (t, J = 7.3 Hz, 3 H), 1.25 (t, J = 7.3 Hz, 3 H), 1.30 (t, J = 7.3 Hz, 3 H), 2.52 (dd, J = 14.3, 7.7 Hz, the low-field half is further split into t, J = 1.3 Hz, 2 H), 2.93–2.99 (m, 2 H), 3.98–4.02 (m, 1 H), 4.03 (q, J = 7.3 Hz, 2 H), 4.17 (q, J = 7.3 Hz, 2 H), 4.24 (q, J = 7.3 Hz, 2 H), 5.05–5.11 (m, 2 H), 5.70–5.86 (m, 1 H), 6.14 (dd, J = 3.1, 0.7 Hz, 1 H), 6.26 (dd, J = 3.1, 1.8 Hz, 1 H), 7.29 (dd, J = 1.8, 0.7 Hz, 1 H) ppm. ^{13}C NMR (75 MHz, $CDCl_3$): δ = 13.9 (2 C), 14.0, 35.8, 38.4, 38.6, 60.2, 60.5, 61.2, 61.3, 108.4, 110.0, 118.8, 132.6, 141.7, 152.2, 169.4, 169.7, 171.5 ppm. MS (ESI, Ar): *m*/*z* (%) = 367 (2) $[M + H]^+$, 321 (100), 303 (80), 275 (12), 229 (38), 167 (60). HRMS (ESI, Ar): calcd. for $C_{19}H_{27}O_7$ $[M + H]^+$ 367.1757; found 367.1771.

Diethyl 2-(But-3-enyl)-2-[1-(furan-2-yl)-3-oxobutyl]malonate (7d): Light yellow oil. Yield 75% (263 mg). IR (neat): $\tilde{\nu}$ = 2982 (w), 1728 (s), 1365 (w), 1228 (w) cm^{-1}. ^1H NMR (300 MHz, $CDCl_3$): δ = 1.26 (t, J = 7.1 Hz, 3 H), 1.29 (t, J = 7.1 Hz, 3 H), 1.68–1.79 (m, 1 H), 1.88–2.02 (m, 2 H), 2.07 (s, 3 H), 2.09–2.16 (m, 1 H), 2.97 (dd, J = 17.4, 2.7 Hz, 1 H), 3.14 (dd, J = 17.4, 10.5 Hz, 1 H), 4.10 (dd, J = 10.5, 2.7 Hz, 1 H), 4.16–4.27 (m, 4 H), 4.93–5.02 (m, 2 H), 5.68–5.78 (m, 1 H), 6.12 (d, J = 3.2 Hz, 1 H), 6.25 (dd, J = 3.2, 1.8 Hz, 1 H), 7.26 (d, J = 1.8 Hz, 1 H) ppm. ^{13}C NMR (100 MHz, $CDCl_3$):

δ = 14.2 (2 C), 29.0, 30.2, 33.3, 37.9, 44.8, 60.5, 61.4, 61.6, 108.5, 110.4, 115.1, 137.7, 141.7, 152.8, 170.2, 170.6, 206.2 ppm. MS (ESI, Ar): *m*/*z* (%) = 373 (100) $[M + Na]^+$, 137 (10). HRMS (ESI, Ar): calcd. for $C_{19}H_{26}O_6Na$ $[M + Na]^+$ 373.1627; found 373.1620.

Diethyl 2-(But-3-enyl)-2-[1-(furan-2-yl)-3-oxo-3-phenylpropyl]malonate (7e): Light yellow oil. Yield 69% (285 mg). IR (neat): $\tilde{\nu}$ = 2981 (s), 1732 (s), 1693 (m), 1449 (m), 1015 (m) cm^{-1}. ^1H NMR (300 MHz, $CDCl_3$): δ = 1.25 (t, *J* = 7.1 Hz, 3 H), 1.33 (t, *J* = 7.1 Hz, 3 H), 1.77–1.82 (m, 1 H), 1.95–2.05 (m, 2 H), 2.10–2.17 (m, 1 H), 3.50 (dd, *J* = 17.4, 2.5 Hz, 1 H), 3.76 (dd, *J* = 17.4, 11.0 Hz, 1 H), 4.10 (dd, *J* = 11.0, 2.5 Hz, 1 H), 4.18–4.35 (m, 4 H), 4.93 (dd, *J* = 10.1, 1.8 Hz, 1 H), 5.02 (dd, *J* = 17.0, 1.8 Hz, 1 H), 5.70–5.80 (m, 1 H), 6.13 (d, *J* = 3.2 Hz, 1 H), 6.22 (dd, *J* = 3.2, 1.8 Hz, 1 H), 7.24 (d, *J* = 1.8 Hz, 1 H), 7.41–7.45 (m, 2 H), 7.51–7.55 (m, 1 H), 7.93–7.95 (m, 2 H) ppm. ^{13}C NMR (100 MHz, $CDCl_3$): δ = 14.0 (2 C), 28.8, 33.3, 37.9, 39.9, 60.5, 61.2, 61.4, 108.3, 110.1, 114.9, 128.0, 128.4, 132.9, 136.8, 137.5, 141.5, 152.6, 170.2, 170.6, 197.5 ppm. MS (ESI, Ar): *m*/*z* (%) = 435 (9) $[M + Na]^+$, 199 (100). HRMS (ESI, Ar): calcd. for $C_{24}H_{28}O_6Na$ $[M + Na]^+$ 435.1784; found 435.1804.

Triethyl 2-(Furan-2-yl)hept-6-ene-1,3,3-tricarboxylate (7f): Light yellow oil. Yield 45% (172 mg). IR (neat): $\tilde{\nu}$ = 2982 (w), 1732 (s), 1021 (w) cm^{-1}. ^1H NMR (400 MHz, $CDCl_3$): δ = 1.15 (t, *J* = 7.1 Hz, 3 H), 1.26 (t, *J* = 7.1 Hz, 3 H), 1.29 (t, *J* = 7.1 Hz, 3 H), 1.67–2.14 (m, 6 H), 2.92–2.94 (m, 1 H), 4.04 (q, *J* = 7.1 Hz, 2 H), 4.22 (two overlapped ABq, *J* = 7.1 Hz, 4 H), 4.93–5.02 (m, 2 H), 5.68–5.78 (m, 1 H), 6.13 (d, *J* = 3.2 Hz, 1 H), 6.27 (dd, *J* = 3.2, 1.8 Hz, 1 H), 7.29 (d, *J* = 1.8 Hz, 1 H) ppm. ^{13}C NMR (100 MHz, $CDCl_3$): δ = 14.2 (2 C), 14.3, 29.0, 33.5, 36.2, 39.3, 60.5, 60.6, 61.5, 61.6, 108.5, 110.3, 115.1, 137.7, 141.9, 152.6, 170.0, 170.6, 172.0 ppm. MS (ESI, Ar): *m*/*z* (%) = 403 (100) $[M + Na]^+$. HRMS (ESI, Ar): calcd. for $C_{20}H_{28}O_7Na$ $[M + Na]^+$ 403.1733; found 403.1741.

General Procedure for the Michael Addition of Diallylamine (10) to Acrylates 1d,e: To a stirred mixture of diallylamine (**10**, 97 mg, 1 mmol) in THF (5 mL) at –78 °C under nitrogen was added *n*BuLi (0.63 mL, 1.6 M solution in hexanes, 1 mmol) dropwise over 20 min. After the addition was complete, the reaction mixture was brought slowly to 0 °C and stirred for another 30 min at the same temperature. The reaction mixture was cooled to –78 °C, and a solution of **1d** (166 mg, 1 mmol) or **1e** (238 mg, 1 mmol) in THF (5 mL) was added dropwise to the reaction mixture. After the addition was complete, the reaction mixture was stirred at –78 °C for another 4 h. The reaction mixture was then quenched with saturated aqueous NH_4Cl. The aqueous layer was extracted with ethyl acetate (3 × 15 mL). The combined organic layers were then washed with brine (20 mL), dried with anhydrous Na_2SO_4 and concentrated in vacuo. The crude residue was then purified by silica gel chromatography with ethyl acetate/*n*-hexane (1:25) as the eluent to afford pure **11d** or **11e**.

Ethyl 3-(Diallylamino)-3-(furan-2-yl)propanoate (11d): Light yellow oil. Yield 79% (209 mg). IR (neat): $\tilde{\nu}$ = 3078 (w), 2980 (s), 2938 (m), 2816 (m), 1738 (s), 1288 (m), 1165 (s) cm^{-1}. ^1H NMR (400 MHz, $CDCl_3$): δ = 1.24 (t, *J* = 7.3 Hz, 3 H), 2.76–2.80 (m, 2 H), 2.81 (ABq, *J* = 14.7, high-field half and low-field half were further split into d, *J* = 6.9 and 8.7 Hz, respectively, 1 H), 2.90 (dd, *J* = 14.7, 8.7 Hz, 1 H), 3.24–3.29 (m, 2 H), 4.09–4.16 (m, 2 H), 4.45 (t, *J* = 7.8 Hz, 1 H), 5.10–5.19 (m, 4 H), 5.71–5.81 (m, 2 H), 6.13 (d, *J* = 3.0 Hz, 1 H), 6.32 (dd, *J* = 3.0, 1.8 Hz, 1 H), 7.37 (d, *J* = 1.8 Hz, 1 H) ppm. ^{13}C NMR (100 MHz, $CDCl_3$): δ = 13.9, 36.4, 53.2 (2 C), 60.0, 107.4, 109.5, 116.6, 136.6, 141.5, 153.0, 170.8 ppm. MS (ESI, Ar): *m*/*z* (%) = 264 (100) $[M + H]^+$, 167 (22), 125 (15), 97 (15). HRMS (ESI, Ar): calcd. for $C_{15}H_{22}NO_3$ $[M + H]^+$ 264.1600; found 264.1593.

Diallyl 2-[1-(Furan-2-yl)-3-oxobutyl]malonate (15): To a stirred mixture of **1a** (136 mg, 1 mmol) and diallyl malonate (**14**, 276 mg, 1.5 mmol) in THF (10 mL) was added DBU (0.075 mL, 76 mg, 0.5 mmol). The reaction mixture was stirred for 6 h. The reaction mixture was then diluted with water and acidified with HCl (10%, 10 mL). The aqueous layer was extracted with ethyl acetate (3 × 15 mL). The combined organic layers were then washed with brine (15 mL), dried with anhydrous Na_2SO_4 and concentrated in vacuo. The crude residue was then purified by silica gel chromatography with ethyl acetate/*n*-hexane (1:20) as the eluent to afford pure **15**. Light yellow oil. Yield 72% (232 mg). IR (neat): $\tilde{\nu}$ = 3058 (m), 2988 (m), 2950 (m), 1733 (s), 1267 (s), 1153 (s) cm^{-1}. ^1H NMR (400 MHz, $CDCl_3$): δ = 2.11 (s, 3 H), 2.98 (ABq, *J* = 17.2, high-field half and low-field half were further split into d, *J* = 5.1 and 8.4 Hz, respectively, 2 H), 3.87 (d, *J* = 7.7 Hz, 1 H), 4.13 (ddd, *J* = 8.4, 7.7, 5.1 Hz, 1 H), 4.53 (dt, *J* = 5.9, 1.5 Hz, 2 H), 4.62 (dt, *J* = 5.9, 1.5 Hz, 2 H), 5.18–5.33 (m, 4 H), 5.73–5.93 (m, 2 H), 6.11 (dd, *J* = 3.3, 0.7 Hz, 1 H), 6.25 (dd, *J* = 3.3, 1.8 Hz, 1 H), 7.28 (dd, *J* = 1.8, 0.7 Hz, 1 H) ppm. ^{13}C NMR (75 MHz, $CDCl_3$): δ = 30.1, 34.0, 44.4, 54.9, 66.2 (2 C), 107.1, 110.3, 118.8 (2 C), 131.4 (2 C), 141.7, 153.4, 167.3, 167.5, 205.7 ppm. MS (ESI, Ar): *m*/*z* (%) = 343 (100) $[M + Na]^+$, 263 (4), 205 (6). HRMS (ESI, Ar): calcd. for $C_{17}H_{20}O_6Na$ $[M + Na]^+$ 343.1158; found 343.1158.

General Procedure for the IMDAF Reaction of Michael Adducts 3, 7 and 11: A solution of the Michael adduct **3**, **7** or **11** (1 mmol) in dry toluene or xylene (10 mL) was refluxed for the specified time (see Tables 1, 2, and 3). The reaction mixture was then cooled to room temperature and concentrated in vacuo. The crude residue was purified, and the two isomers, if any, were separated by silica gel column chromatography with ethyl acetate/*n*-hexane (1:10 to 1:5) as the eluent.

Compounds 4a and 5a

4a: Colorless solid. Yield 58% (122 mg). M.p. 62 °C. R_f = 0.32 (EtOAc/*n*-hexane, 1:4). IR (KBr): $\tilde{\nu}$ = 3012 (m), 2937 (m), 2873 (m), 1712 (s), 1384 (s), 1312 (m), 1164 (m) cm^{-1}. ^1H NMR (300 MHz, $CDCl_3$): δ = 1.51 (dd, *J* = 11.7, 7.3 Hz, 1 H), 1.79 (ddd, *J* = 11.7, 4.8, 2.6 Hz, 1 H), 2.15 (s, 3 H), 2.31 (dddd, *J* = 10.4, 7.7, 7.3, 2.6 Hz, 1 H), 2.75 (dd collapsed to t, *J* = 10.4 Hz, 1 H), 2.85 (dd, *J* = 18.3, 8.8 Hz, 1 H), 3.01 (dd, *J* = 10.4, 7.7 Hz, 1 H), 3.08 (dd, *J* = 18.3, 5.2 Hz, 1 H), 4.22 (unresolved dd, *J* = 8.8, 5.2 Hz, 1 H), 5.03 (dd, *J* = 4.8, 1.5 Hz, 1 H), 6.30 (d, *J* = 5.8 Hz, 1 H), 6.40 (dd, *J* = 5.8, 1.5 Hz, 1 H) ppm. These data were confirmed by a ^1H-^1H COSY experiment (see also Table S2). ^{13}C NMR (75 MHz, $CDCl_3$): δ = 30.1, 34.7, 36.6, 41.0, 46.4, 48.2, 79.7, 100.4, 136.0, 137.5, 206.9 ppm. MS (ESI, Ar): *m*/*z* (%) = 233 (82) $[M + Na]^+$, 193 (98), 151 (100), 135 (22). HRMS (ESI, Ar): calcd. for $C_{11}H_{14}O_2NaS$ $[M + Na]^+$ 233.0612; found 233.0617.

5a: Light yellow oil. Yield 9% (19 mg). R_f = 0.23 (EtOAc/*n*-hexane, 1:4). IR (neat): $\tilde{\nu}$ = 2924 (s), 2855 (m), 1709 (s), 1368 (m), 1321 (m), 1167 (m) cm^{-1}. ^1H NMR (300 MHz, $CDCl_3$): δ = 1.51 (dd, *J* = 11.3, 7.3 Hz, 1 H), 1.77 (ddd, *J* = 11.3, 4.4, 2.6 Hz, 1 H), 2.23 (s, 3 H), 2.29 (dddd, *J* = 11.0, 7.7, 7.3, 2.6 Hz, 1 H), 2.73 (dd collapsed to t, *J* = 11.0 Hz, 1 H), 2.86 (dd, *J* = 17.2, 9.9 Hz, 1 H), 3.05 (dd, *J* = 11.0, 7.7 Hz, 1 H), 3.13 (dd, *J* = 17.2, 5.1 Hz, 1 H), 3.97 (dd, *J* = 9.9, 5.1 Hz, 1 H), 5.04 (dd, *J* = 4.4, 1.6 Hz, 1 H), 6.28 (d, *J* = 5.8 Hz, 1 H), 6.46 (dd, *J* = 5.8, 1.6 Hz, 1 H) ppm. These data were confirmed by ^1H-^1H COSY experiment (see also Table S3). ^{13}C NMR (75 MHz, $CDCl_3$): δ = 30.3, 34.5, 36.7, 42.2, 47.3, 49.6, 79.5, 101.8, 133.5, 138.1, 205.6 ppm. MS (ESI, Ar): *m*/*z*

(%) = 233 (100) $[M + Na]^+$, 193 (12), 151 (70). HRMS (ESI, Ar): calcd. for $C_{11}H_{14}O_2NaS$ $[M + Na]^+$ 233.0612; found 233.0608.

Compounds 4b and 5b

4b: Colorless solid. Yield 51% (139 mg). M.p. 73 °C. R_f = 0.27 (EtOAc/*n*-hexane, 1:4). IR (KBr): $\tilde{\nu}$ = 3056 (w), 2938 (w), 1683 (s), 1591 (m), 1321 (m), 1268 (m) cm^{-1}. ^1H NMR (300 MHz, $CDCl_3$): δ = 1.53 (dd, J = 11.7, 7.3 Hz, 1 H), 1.82 (ddd, J = 11.7, 4.4, 2.6 Hz, 1 H), 2.38 (dddd, J = 10.6, 7.7, 7.3, 2.6 Hz, 1 H), 2.78 (dd collapsed to t, J = 10.6 Hz, 1 H), 3.07 (dd, J = 10.6, 7.7 Hz, 1 H), 3.51 (ABq, J = 18.3 Hz, high-field and low-field halves were further split into d, J = 8.8 and 4.8 Hz, respectively, 2 H), 4.45 (dd, J = 8.8, 4.8 Hz, 1 H), 5.06 (dd, J = 4.4, 1.6 Hz, 1 H), 6.39 (ABq, J = 5.9 Hz, the low-field half was further split into d, J = 1.6 Hz, 2 H), 7.41–7.44 (m, 2 H), 7.46–7.58 (m, 1 H), 7.97–7.99 (m, 2 H) ppm. These data were confirmed by ^1H-^1H COSY and NOESY experiments (see also Table S4). ^{13}C NMR (75 MHz, $CDCl_3$): δ = 34.5, 36.5, 41.2, 41.9, 48.0, 79.5, 100.3, 127.9, 128.3, 132.9, 135.8, 136.2, 137.4, 197.8 ppm. MS (ESI, Ar): m/z (%) = 295 (100) $[M + Na]^+$, 255 (28), 105 (25). HRMS (ESI, Ar): calcd. for $C_{16}H_{16}O_2NaS$ $[M + Na]^+$ 295.0769; found 295.0775.

5b: Colorless solid. Yield 8% (22 mg). M.p. 130 °C. R_f = 0.14 (EtOAc/*n*-hexane, 1:4). IR (KBr): $\tilde{\nu}$ = 3020 (w), 2920 (w), 1673 (s), 1593 (m), 1446 (m), 1211 (m) cm^{-1}. ^1H NMR (300 MHz, $CDCl_3$): δ = 1.53 (dd, J = 11.7, 7.7 Hz, 1 H), 1.80 (ddd, J = 11.7, 4.4, 2.6 Hz, 1 H), 2.35 (dddd collapsed to ddd, J = 10.8, 7.7, 2.6 Hz, 1 H), 2.75 (dd collapsed to t, J = 10.8 Hz, 1 H), 3.06 (dd, J = 10.8, 7.7 Hz, 1 H), 3.55 (ABq, J = 17.2 Hz, high-field and low-field halves were further split into d, J = 9.2 and 5.3 Hz, respectively, 2 H), 4.20 (dd, J = 9.2, 5.3 Hz, 1 H), 5.05 (dd, J = 4.4, 1.8 Hz, 1 H), 6.35 (d, J = 5.9 Hz, 1 H), 6.46 (dd, J = 5.9, 1.8 Hz, 1 H), 7.45–7.50 (m, 2 H), 7.56–7.61 (m, 1 H), 7.98–7.99 (m, 2 H) ppm. These data were confirmed by ^1H-^1H COSY and NOESY experiments (see also Table S5). ^{13}C NMR (75 MHz, $CDCl_3$): δ = 34.5, 36.8, 42.5, 44.7, 47.4, 79.5, 101.9, 128.1, 128.7, 133.4, 133.7, 136.5, 137.9, 197.0 ppm. MS (ESI, Ar): m/z (%) = 295 (100) $[M + Na]^+$, 255 (4), 135 (10), 105 (25), 77 (4). HRMS (ESI, Ar): calcd. for $C_{16}H_{16}O_2NaS$ $[M + Na]^+$ 295.0769; found 295.0770.

Compound 4c: Colorless solid. Yield 44% (111 mg). M.p. 109 °C. R_f = 0.27 (EtOAc/*n*-hexane, 1:4). IR (neat): $\tilde{\nu}$ = 2938 (m), 1725 (s), 1694 (m), 1250 (m) cm^{-1}. ^1H NMR (400 MHz, $CDCl_3$): δ = 1.46 (dd, J = 11.7, 7.3 Hz, 1 H), 1.75 (ddd, J = 11.7, 4.4, 2.6 Hz, 1 H), 2.25 (s, 6 H), 2.27–2.38 (m, 1 H), 2.70 (dd collapsed to t, J = 10.6 Hz, 1 H), 2.96 (dd, J = 10.6, 7.3 Hz, 1 H), 4.29 (d, J = 11.2 Hz, 1 H), 4.50 (d, J = 11.2 Hz, 1 H), 5.02 (dd, J = 4.4, 1.6 Hz, 1 H), 6.27 (unresolved br. s, 2 H) ppm. These data were confirmed by ^1H-^1H COSY experiment (see also Table S6). ^{13}C NMR (75 MHz, $CDCl_3$): δ = 29.5, 31.4, 34.1, 36.4, 45.3, 49.4, 71.5, 79.9, 99.3, 135.6, 137.0, 200.9, 202.1 ppm. MS (ESI, Ar): m/z (%) = 275 (4) $[M + Na]^+$, 193 (100). HRMS (ESI, Ar): calcd. for $C_{13}H_{16}O_3NaS$ $[M + Na]^+$ 275.0718; found 275.0725. The minor isomer **5c** could not be isolated in pure form.

Compounds 8a and 9a

8a: Light yellow oil. Yield 61% (206 mg). R_f = 0.29 (EtOAc/*n*-hexane, 1:4). IR (neat): $\tilde{\nu}$ = 3056 (m), 2986 (m), 1725 (br., s), 1266 (s) cm^{-1}. ^1H NMR (400 MHz, $CDCl_3$): δ = 1.25 (two overlapped t, J = 7.3 Hz, 6 H), 1.45 (dd, J = 11.4, 7.7 Hz, 1 H), 1.70 (ddd, J = 11.4, 4.4, 3.3 Hz, 1 H), 1.79 (dddd, J = 9.9, 8.1, 7.7, 3.3 Hz, 1 H), 2.12 (s, 3 H), 2.36 (ABq, J = 13.2 Hz, the low-field and high-field halves were further split into d, J = 9.9 and 8.1 Hz, respectively, 2 H), 2.55 (dd, J = 17.2, 4.8 Hz, 1 H), 2.80 (dd, J = 17.2, 10.3 Hz, 1 H), 3.90 (dd, J = 10.3, 4.8 Hz, 1 H), 4.10–4.28 (m, 4 H), 4.93 (dd, J = 4.4, 1.8 Hz, 1 H), 6.16 (d, J = 5.9 Hz, 1 H), 6.40 (dd, J = 5.9, 1.8 Hz, 1 H) ppm. These data were confirmed by ^1H-^1H COSY experiment (see also Table S7). ^{13}C NMR (100 MHz, $CDCl_3$): δ = 13.8 (2 C), 30.1, 33.0, 38.5, 39.4, 40.2, 40.9, 61.1, 61.5, 65.1, 79.3, 98.1, 134.2, 137.2, 169.7, 171.8, 206.3 ppm. MS (ESI, Ar): m/z (%) = 359 (100) $[M + Na]^+$, 273 (8), 189 (10), 159 (18). HRMS (ESI, Ar): calcd. for $C_{18}H_{24}O_6Na$ $[M + Na]^+$ 359.1471; found 359.1469.

9a: Light yellow oil. Yield 12% (41 mg). R_f = 0.13 (EtOAc/*n*-hexane, 1:4). IR (neat): $\tilde{\nu}$ = 3057 (m), 2986 (m), 1727 (m), 1266 (s) cm^{-1}. ^1H NMR (400 MHz, $CDCl_3$): δ = 1.26 (two overlapped t, J = 7.3 Hz, 6 H), 1.42 (dd, J = 11.4, 7.7 Hz, 1 H), 1.68 (ddd, J = 11.4, 4.4, 3.3 Hz, 1 H), 1.99 (dd, J = 13.2, 11.4 Hz, 1 H), 2.02–2.20 (m, 1 H), 2.21 (s, 3 H), 2.53 (dd, J = 13.2, 7.0 Hz, 1 H), 2.91 (d, J = 7.3 Hz, 2 H), 3.45 (dd collapsed to t, J = 7.3 Hz, 1 H), 4.12–4.23 (m, 4 H), 4.98 (dd, J = 4.4, 1.5 Hz, 1 H), 6.24 (ABq, J = 5.9 Hz, the high-field half was further split into d, J = 1.5 Hz, 2 H) ppm. These data were confirmed by ^1H-^1H COSY experiment (see also Table S8). ^{13}C NMR (100 MHz, $CDCl_3$): δ = 14.0 (2 C), 29.7, 32.3, 39.2, 41.9, 43.0, 43.2, 61.4 (2 C), 66.9, 79.8, 99.6, 134.3, 135.6, 170.9, 171.2, 206.4 ppm. MS (ESI, Ar): m/z (%) = 359 (100) $[M + Na]^+$, 273 (53), 189 (22), 159 (11), 61 (8). HRMS (ESI, Ar): calcd. for $C_{18}H_{24}O_6Na$ $[M + Na]^+$ 359.1471; found 359.1467.

Compounds 8b and 9b

8b: Colorless solid. Yield 71% (283 mg). M.p. 105 °C. R_f = 0.33 (EtOAc/*n*-hexane, 1:4). IR (KBr): $\tilde{\nu}$ = 3057 (w), 2985 (w), 1726 (br., s), 1266 (s) cm^{-1}. ^1H NMR (400 MHz, $CDCl_3$): δ = 1.19 (t, J = 7.1 Hz, 3 H), 1.26 (t, J = 7.1 Hz, 3 H), 1.46 (dd, J = 11.7, 7.8 Hz, 1 H), 1.72 (ddd collapsed to dt, J = 11.7, 4.4 Hz, 1 H), 1.86 (dddd collapsed to ddd, J = 8.8, 7.8, 4.4 Hz, 1 H), 2.40 (ABqd, J = 13.2, 8.8 Hz, 2 H), 3.11 (dd, J = 17.8, 4.9 Hz, 1 H), 3.39 (dd, J = 17.8, 10.0 Hz, 1 H), 4.00 (dd, J = 10.0, 4.9 Hz, 1 H), 4.21 (m, 4 H), 4.92 (dd, J = 4.4, 1.5 Hz, 1 H), 6.15 (dd, J = 5.9, 1.5 Hz, 1 H), 6.46 (d, J = 5.9 Hz, 1 H), 7.40–7.45 (m, 2 H), 7.50–7.55 (m, 1 H), 7.93–7.96 (m, 2 H) ppm. These data were confirmed by ^1H-^1H COSY and NOESY experiments (see also Table S9). ^{13}C NMR (100 MHz, $CDCl_3$): δ = 14.0 (2 C), 33.4, 36.0, 39.0, 39.9, 41.1, 61.3, 61.7, 65.4, 79.5, 98.5, 128.1, 128.4, 132.8, 134.7, 137.0, 137.1, 170.2, 172.1, 197.9 ppm. MS (ESI, Ar): m/z (%) = 421 (100) $[M + Na]^+$, 335 (50), 263 (20), 261 (54). HRMS (ESI, Ar): calcd. for $C_{23}H_{26}O_6Na$ $[M + Na]^+$ 421.1627; found 421.1638. Selected X-ray data: $C_{23}H_{26}O_6$, M = 398.44, orthorhombic, $P2_12_12_1$, a = 8.3315(6) Å, b = 13.9919(14) Å, c = 18.2911(15) Å, V = 2132.3(3) $Å^3$, Z = 4, $D_{calcd.}$ = 1.241 $g\,cm^{-3}$, μ = 0.089 mm^{-1}, size = 0.40 × 0.35 × 0.30 mm, GOF = 0.922. Reflections collected: unique 9669/3730 [R(int) = 0.0325]. Final R indices [$I > 2\sigma(I)$]: R_1 = 0.0488, wR_2 = 0.1118; R indices (all data): R_1 = 0.1069, wR_2 = 0.1335 (see also Table S17).

9b: Light yellow oil. Yield 16% (64 mg). R_f = 0.16 (EtOAc/*n*-hexane, 1:4). IR (neat): $\tilde{\nu}$ = 3055 (m), 2985 (w), 1725 (br., s), 1686 (m), 1265 (s) cm^{-1}. ^1H NMR (300 MHz, $CDCl_3$): δ = 1.23 (t, J = 7.3 Hz, 6 H), 1.43 (dd, J = 11.2, 7.8 Hz, 1 H), 1.72 (ddd collapsed to dt, J = 11.2, 4.4 Hz, 1 H), 2.02–2.06 (m, 2 H), 2.21–2.29 (m, 1 H), 2.57 (dd, J = 12.9, 6.6 Hz, 1 H), 3.47–3.67 (m, 2 H), 4.10–4.25 (m, 4 H), 4.99 (dd, J = 4.4, 1.5 Hz, 1 H), 6.21 (dd, J = 5.9, 1.5 Hz, 1 H), 6.23 (ABq, J = 5.9 Hz, 1 H), 7.44–7.49 (m, 2 H), 7.54–7.59 (m, 1 H), 8.00–8.02 (m, 2 H) ppm. These data were confirmed by ^1H-^1H COSY and NOESY experiments (see also Table S10). ^{13}C NMR (75 MHz, $CDCl_3$): δ = 14.1, 29.7, 32.4, 38.0, 39.4, 42.0, 43.1, 61.5 (2 C), 67.0, 79.9, 99.8, 128.2, 128.7, 133.2, 134.8, 135.4, 136.8, 171.0, 171.5, 197.6 ppm. MS (ESI, Ar): m/z (%) = 421 (100) $[M + Na]^+$, 335 (30), 261 (12). HRMS (ESI, Ar): calcd. for $C_{23}H_{26}O_6Na$ $[M + Na]^+$ 421.1627; found 421.1643.

Compounds 8c and 9c

8c: Colorless oil. Yield 65% (238 mg). R_f = 0.29 (EtOAc/*n*-hexane, 1:4). IR (neat): $\tilde{\nu}$ = 3056 (m), 2986 (m), 1729 (br., s), 1266 (s) cm^{-1}. ^1H NMR (300 MHz, $CDCl_3$): δ = 1.24 (three overlapped t, J = 7.3 Hz, 9 H), 1.44 (dd, J = 11.4, 7.7 Hz, 1 H), 1.70 (ddd, J = 11.4, 4.4, 3.3 Hz, 1 H), 1.76–1.85 (m, 1 H), 2.35–2.39 (m, 2 H), 2.53–2.56 (m, 2 H), 3.90 (dd, J = 9.2, 6.6 Hz, 1 H), 4.06–4.28 (three overlapped q, J = 7.3 Hz, 6 H), 4.97 (dd, J = 4.4, 1.5 Hz, 1 H), 6.19 (dd, J = 5.9, 1.5 Hz, 1 H), 6.41 (d, J = 5.9 Hz, 1 H) ppm. These data were confirmed by ^1H-^1H COSY experiment (see also Table S11). ^{13}C NMR (100 MHz, $CDCl_3$): δ = 13.8 (2 C), 13.9, 31.7, 32.9, 38.5, 40.2, 40.9, 60.1, 61.1, 61.5, 65.2, 79.4, 97.9, 134.5, 136.9, 169.4, 171.7, 171.8 ppm. MS (ESI, Ar): *m*/*z* (%) = 389 (100) $[M + Na]^+$, 303 (24), 229 (9). HRMS (ESI, Ar): calcd. for $C_{19}H_{26}O_7Na$ $[M + Na]^+$ 389.1576; found 389.1581.

9c: Light yellow oil. Yield 12% (45 mg). R_f = 0.13 (EtOAc/*n*-hexane, 1:4). IR (neat): $\tilde{\nu}$ = 3055 (m), 2985 (w), 1729 (br., s), 1266 (s) cm^{-1}. ^1H NMR (400 MHz, $CDCl_3$): δ = 1.26 (three overlapped t, J = 7.0 Hz, 9 H), 1.42 (dd, J = 11.4, 7.7 Hz, 1 H), 1.67 (ddd collapsed to dt, J = 11.4, 4.3 Hz, 1 H), 1.97 (dd, J = 12.8, 11.4 Hz, 1 H), 2.17–2.27 (dddd, J = 11.4, 7.7, 7.0, 4.3 Hz, 1 H), 2.53 (dd, J = 12.8, 7.0 Hz, 1 H), 2.80 (ABq, J = 16.5 Hz, the high-field and low-field halves were further split to d, J = 9.9 and 5.5 Hz, respectively, 2 H), 3.43 (dd, J = 9.9, 5.5 Hz, 1 H), 4.18 (three overlapped q, J = 7.0 Hz, 6 H), 4.98 (dd, J = 4.3, 1.8 Hz, 1 H), 6.25 (dd, J = 5.9, 1.8 Hz, 1 H), 6.35 (d, J = 5.9 Hz, 1 H) ppm. These data were confirmed by ^1H-^1H COSY experiment (see also Table S12). ^{13}C NMR (75 MHz, $CDCl_3$): δ = 14.0 (2 C), 14.2, 32.4, 34.0, 39.3, 42.6, 43.0, 60.7 (2 C), 61.5, 66.9, 79.8, 99.6, 134.3, 135.5, 170.8, 171.1, 171.7 ppm. MS (ESI, Ar): *m*/*z* (%) = 389 (100) $[M + Na]^+$, 303 (94), 229 (73), 201 (25). HRMS (ESI, Ar): calcd. for $C_{19}H_{26}O_7Na$ $[M + Na]^+$ 389.1576; found 389.1577.

Compound 8d: Light yellow oil. Yield 41% (145 mg). R_f = 0.39 (EtOAc/*n*-hexane, 1:4). IR (neat): $\tilde{\nu}$ = 2926 (w), 1732 (s), 1254 (s), 1098 (w) cm^{-1}. ^1H NMR (400 MHz, $CDCl_3$): δ = 1.26 (t, J = 7.3 Hz, 6 H), 1.36 (ddd, J = 11.7, 4.4, 2.0 Hz, 1 H), 1.45–1.57 (m, 3 H), 1.79–1.93 (m, 2 H), 2.12 (s, 3 H), 2.37–2.43 (m, 1 H), 3.06–3.09 (m, 2 H), 3.50 (dd, J = 5.9, 3.9 Hz, 1 H), 4.07–4.28 (m, 4 H), 4.86 (dd, J = 4.4, 1.5 Hz, 1 H), 5.86 (d, J = 5.9 Hz, 1 H), 6.25 (dd, J = 5.9, 1.5 Hz, 1 H) ppm. These data were confirmed by ^1H-^1H COSY experiment. ^{13}C NMR (100 MHz, $CDCl_3$): δ = 14.1, 28.0, 29.8, 30.3, 32.8, 35.2, 36.2, 36.8, 43.9, 57.2, 61.0, 61.8, 78.7, 89.1, 136.4, 137.5, 170.1, 172.1, 208.1 ppm. MS (ESI, Ar): *m*/*z* (%) = 373 (100) $[M + Na]^+$, 287 (10), 241 (38), 215 (50), 195 (30). HRMS (ESI, Ar): calcd. for $C_{19}H_{26}O_6Na$ $[M + Na]^+$ 373.1627; found 373.1632.

Compounds 8e and 9e

8e: Colorless solid. Yield 40% (166 mg). M.p. 99 °C. R_f = 0.37 (EtOAc/*n*-hexane, 1:4). IR (neat): $\tilde{\nu}$ = 2979 (w), 2928 (w), 1732 (s), 1688 (m), 1449 (m), 1254 (m), 1096 (m) cm^{-1}. ^1H NMR (400 MHz, $CDCl_3$): δ = 1.09 (t, J = 7.0 Hz, 3 H), 1.31 (t, J = 7.0 Hz, 3 H), 1.39 (ddd, J = 11.0, 4.4, 2.6 Hz, 1 H), 1.47–1.63 (m, 2 H), 1.65–1.70 (m, 1 H), 1.88–1.92 (m, 2 H), 2.41–2.48 (m, 1 H), 3.63–3.65 (m, 2 H), 3.79 (dd, J = 5.9, 3.7 Hz, 1 H), 3.96–4.14 (m, 2 H), 4.27 (q, J = 7.0 Hz, 2 H), 4.87 (dd, J = 4.4, 1.5 Hz, 1 H), 5.91 (d, J = 5.5 Hz, 1 H), 6.21 (dd, J = 5.5, 1.5 Hz, 1 H), 7.40–7.46 (m, 2 H), 7.51–7.56 (m, 1 H), 8.00–8.02 (m, 2 H) ppm. These data were confirmed by ^1H-^1H COSY experiment. ^{13}C NMR (75 MHz, $CDCl_3$): δ = 13.9, 14.1, 27.9, 32.8, 35.2, 36.1, 36.8, 38.9, 57.2, 60.9, 61.6, 78.6, 89.2, 128.2, 128.4, 132.9, 136.4, 137.0, 137.3, 170.1, 171.9, 199.1 ppm. MS (ESI, Ar): *m*/*z* (%) = 413 (2) $[M + H]^+$, 395 (100). HRMS (ESI, Ar): calcd. for $C_{24}H_{29}O_6$ $[M + H]^+$ 413.1964; found 413.1971. Selected X-ray data: $C_{24}H_{28}O_6$: M = 412.46, triclinic, $P\bar{1}$, a = 8.9557(3) Å, b = 9.8870(4) Å, c = 13.4143(5) Å, V = 1070.23(7) $Å^3$, Z = 2, $D_{calcd.}$ = 1.280 $g\,cm^{-3}$, μ = 0.091 mm^{-1}, size = 0.23 × 0.18 × 0.16 mm, *GOF* = 1.047. Reflections collected: unique 9289/3766 [R(int)] = 0.0206. Final R indices [$I > 2\sigma(I)$]: R_1 = 0.0379, wR_2 = 0.0930; R indices (all data): R_1 = 0.0565, wR_2 = 0.0984 (see also Table S17).

9e: Light yellow oil. Yield 3% (13 mg). R_f = 0.23 (EtOAc/*n*-hexane, 1:4) IR (neat): $\tilde{\nu}$ = 2929 (s), 1732 (s), 1260 (m) cm^{-1}. ^1H NMR (400 MHz, $CDCl_3$): δ = 1.16 (t, J = 7.0 Hz, 3 H), 1.17 (t, J = 7.0 Hz, 3 H), 1.22–1.55 (m, 2 H), 1.56–1.65 (m, 2 H), 1.87–1.94 (m, 1 H), 2.02–2.13 (m, 1 H), 2.43–2.49 (m, 1 H), 3.18 (dd, J = 18.5, 5.9 Hz, 1 H), 3.49 (dd, J = 18.5, 4.4 Hz, 1 H), 3.96–4.00 (m, 1 H), 4.01–4.22 (two overlapped q, J = 7.0 Hz, 4 H), 4.81 (dd, J = 4.4, 1.8 Hz, 1 H), 6.11 (d, J = 5.9 Hz, 1 H), 6.31 (dd, J = 5.9, 1.8 Hz, 1 H), 7.43–7.48 (m, 2 H), 7.53–7.55 (m, 1 H), 7.97–8.01 (m, 2 H) ppm. These data were confirmed by ^1H-^1H COSY experiment. ^{13}C NMR (100 MHz, $CDCl_3$): δ = 14.0, 14.1, 26.8, 27.9, 33.2, 35.2, 35.5, 39.3, 57.2, 61.7 (2 C), 78.1, 90.3, 128.2, 128.8, 133.2, 135.8, 137.1, 137.7, 170.4, 171.9, 197.2 ppm. MS (ESI, Ar): *m*/*z* (%) = 413 (2) $[M + H]^+$, 395 (100). HRMS (ESI, Ar): calcd. for $C_{24}H_{29}O_6$ $[M + H]^+$ 413.1964; found 413.1957.

Compounds 12d and 13d

12d: Light yellow oil. Yield 20% (53 mg). R_f = 0.19 (EtOAc/*n*-hexane, 1:5). IR (KBr): $\tilde{\nu}$ = 3076 (w), 2980 (w), 2938 (w), 2867 (w), 1735 (s), 1180 (m) cm^{-1}. ^1H NMR (300 MHz, $CDCl_3$): δ = 1.25 (t, J = 7.3 Hz, 3 H), 1.48 (dd, J = 11.7, 7.8 Hz, 1 H), 1.72 (ddd collapsed to dt, J = 11.7, 4.4 Hz, 1 H), 2.06 (dtd, J = 10.7, 7.8, 4.4 Hz, 1 H), 2.64–2.66 (m, 2 H), 2.83 (dd, J = 10.7, 7.8 Hz, 1 H), 2.90 (dd collapsed to t, J = 10.7 Hz, 1 H), 3.15 (dd, J = 14.1, 7.3 Hz, 1 H), 3.43 (ddt, J = 13.7, 5.9, 1.5 Hz, 1 H), 3.64 (dd collapsed to t, J = 6.8 Hz, 1 H), 4.13 (q, J = 7.3 Hz, 2 H), 5.05 (dd, J = 4.4, 1.5 Hz, 1 H), 5.13 (d, J = 10.2 Hz, 1 H), 5.21 (dd, J = 17.1, 1.5 Hz, 1 H), 5.85–5.98 (m, 1 H), 6.26 (dd, J = 5.9, 1.5 Hz, 1 H), 6.40 (d, J = 5.9 Hz, 1 H) ppm. These data were confirmed by ^1H-^1H COSY experiment (see also Table S13). ^{13}C NMR (100 MHz, $CDCl_3$): δ = 14.0, 29.5, 32.4, 34.1, 41.1, 56.4, 57.2, 59.1, 60.1, 79.2, 97.9, 117.0, 135.3, 135.5, 172.0 ppm. MS (ESI, Ar): *m*/*z* (%) = 264 (100) $[M + H]^+$, 167 (10), 125 (9), 95 (6). HRMS (ESI, Ar): calcd. for $C_{15}H_{22}NO_3$ $[M + H]^+$ 264.1600; found 264.1599.

13d: Light yellow oil. Yield 69% (182 mg). R_f = 0.37 (EtOAc/*n*-hexane, 1:5). IR (neat): $\tilde{\nu}$ = 3055 (m), 2984 (m), 1730 (s), 1266 (s) cm^{-1}. ^1H NMR (300 MHz, $CDCl_3$): δ = 1.26 (t, J = 7.3 Hz, 3 H), 1.32 (dd, J = 11.5, 7.5 Hz, 1 H), 1.68 (ddd, J = 11.5, 4.4, 2.8 Hz, 1 H), 1.98–2.08 (m, 1 H), 2.17 (dd, J = 10.3, 8.4 Hz, 1 H), 2.71 (ABq, J = 15.8 Hz, the high-field and low-field halves were further split into d, J = 8.4 and 5.1 Hz, respectively, 1 H), 3.14 (dd, J = 13.6, 7.3 Hz, 1 H), 3.23–3.25 (m, 1 H), 3.27–3.30 (m, 1 H), 3.43 (ddt, J = 13.6, 5.9, 1.5 Hz, 1 H), 4.16 (q, J = 7.3 Hz, 2 H), 4.98 (dd, J = 4.4, 1.7 Hz, 1 H), 5.12 (dd, J = 10.3, 0.7 Hz, 1 H), 5.21 (dd, J = 17.2, 1.5 Hz, 1 H), 5.84–5.96 (m, 1 H), 6.30 (dd, J = 5.9, 1.7 Hz, 1 H), 6.41 (d, J = 5.9 Hz, 1 H) ppm. These data were confirmed by ^1H-^1H COSY experiment (see also Table S14). ^{13}C NMR (100 MHz, $CDCl_3$): δ = 13.7, 29.1, 37.7, 41.0, 57.0, 57.9, 59.8, 60.6, 78.9, 98.7, 116.6, 133.6, 135.1, 135.3, 170.6 ppm. MS (ESI, Ar): *m*/*z* (%) = 264 (100) $[M + H]^+$, 167 (40), 125 (80), 97 (69), 95 (54), 81 (25). HRMS (ESI, Ar): calcd. for $C_{15}H_{22}NO_3$ $[M + H]^+$ 264.1600; found 264.1605.

Compounds 12e and 13e

12e: Light yellow oil. Yield 13% (44 mg). R_f = 0.19 (EtOAc/*n*-hexane, 1:5). IR (neat): $\tilde{\nu}$ = 3077 (w), 2926 (w), 1734 (s), 1180 (m)

cm^{-1}. ^{1}H NMR (400 MHz, $CDCl_3$): δ = 1.25 (two overlapped t, J = 6.9 Hz, 6 H), 1.47 (dd, J = 11.6, 7.9 Hz, 1 H), 1.70 (ddd, J = 11.6, 4.4, 3.0 Hz, 1 H), 2.07 (dddd, J = 9.5, 7.9, 7.3, 3.0 Hz, 1 H), 2.63–2.66 (m, 2 H), 2.83 (dd, J = 10.6, 7.3 Hz, 1 H), 2.90 (dd, J = 10.6, 9.5 Hz, 1 H), 3.15 (dd, J = 13.9, 7.3 Hz, 1 H), 3.43 (ddt, J = 13.9, 5.5, 1.5 Hz, 1 H), 3.64 (ABq, J = 6.6 Hz, 1 H), 4.12 (two overlapped q, J = 6.9 Hz, 4 H), 5.05 (dd, J = 4.4, 1.5 Hz, 1 H), 5.16 (dq, J = 17.2, 1.5 Hz, 1 H), 5.85–5.98 (m, 1 H), 6.26 (dd, J = 5.9, 1.5 Hz, 1 H), 6.39 (d, J = 5.9 Hz, 1 H) ppm. These data were confirmed by ^{1}H-^{1}H COSY experiment (see also Table S15). ^{13}C NMR (75 MHz, $CDCl_3$): δ = 14.3, 32.7, 34.3, 41.3, 56.6, 57.5, 59.3, 60.5, 79.4, 98.2, 117.3, 135.5 (2 C), 135.7, 172.3 ppm. MS (ESI, Ar): m/z (%) = 264 [M – CO_2Et + H]$^+$, (100), 167 (22), 125 (25), 95 (18). HRMS (ESI, Ar): calcd. for $C_{15}H_{22}NO_3$ [M – CO_2Et + H]$^+$ 264.1600; found 264.1591.

13e: Light yellow oil. Yield 60% (202 mg). R_f = 0.35 (EtOAc/*n*-hexane, 1:5). IR (neat): $\tilde{\nu}$ = 3054 (m), 2986 (m), 1730 (m), 1266 (s) cm^{-1}. ^{1}H NMR (400 MHz, $CDCl_3$): δ = 1.26 (t, J = 7.0 Hz, 6 H), 1.32 (dd, J = 11.4, 7.5 Hz, 1 H), 1.68 (ddd, J = 11.4, 4.4, 2.9 Hz, 1 H), 2.03 (dddd, J = 13.6, 10.6, 7.5, 2.9 Hz, 1 H), 2.16 (dd, J = 10.6, 8.4 Hz, 1 H), 2.60 (ABq, J = 8.4 Hz, 1 H), 2.74 (dd, J = 15.4, 5.1 Hz, 1 H), 3.13 (dd, J = 13.6, 7.3 Hz, 1 H), 3.22–3.29 (m, 2 H), 3.43 (ddt, J = 13.6, 5.9, 1.6 Hz, 1 H), 4.16 (q, J = 7.0 Hz, 4 H), 4.99 (dd, J = 4.4, 1.5 Hz, 1 H), 5.09–5.21 (m, 1 H), 5.82–5.96 (m, 1 H), 6.29 (dd, J = 5.9, 1.5 Hz, 1 H), 6.41 (d, J = 5.9 Hz, 1 H) ppm. These data were confirmed by ^{1}H-^{1}H COSY experiment (see also Table S16). ^{13}C NMR (75 MHz, $CDCl_3$): δ = 14.2, 29.6, 38.3, 41.6, 57.6, 58.5, 60.4, 61.1, 79.5, 99.2, 117.2, 134.1, 135.6, 135.8, 171.3 ppm. MS (ESI, Ar): m/z (%) = 264 (100) [M – CO_2Et + H]$^+$, 167 (3), 125 (5). HRMS (ESI, Ar): calcd. for $C_{15}H_{22}NO_3$ [M – CO_2Et + H]$^+$) 264.1600; found 264.1602.

Supporting Information (see footnote on the first page of this article): NMR spectroscopic data tables, copies of NMR spectra for all new compounds, RHF/3-21G*- and B3LYP/6-31+G*-calculated coordinates of products and transition states.

Acknowledgments

I. N. N. thanks the Department of Science and Technology, India for financial assistance and the Sophisticated Analytical Instrumentation Facility, Indian Institute of Technology Bombay, for selected NMR spectroscopic data. M. D. thanks the Council of Scientific and Industrial Research, India, and M. K. K. thanks the Department of Atomic Energy-Board of Research in Nuclear Sciences for a research fellowship.

[1] Selected reviews on Type-1 IMDA: a) A. Deagostino, C. Prandi, C. Zavattaro, P. Venturello, *Eur. J. Org. Chem.* **2006**, 2463–2483; b) K.-i. Takao, R. Munakata, K.-i. Tadano, *Chem. Rev.* **2005**, *105*, 4779–4807; c) G. R. Heintzelman, I. R. Meigh, Y. R. Mahajan, S. M. Weinreb, *Org. React.* **2005**, *65*, 141–599; d) L. F. Tietze, N. Rackelmann, *Pure Appl. Chem.* **2004**, *76*, 1967–1983; e) A. Padwa, *Pure Appl. Chem.* **2004**, *76*, 1933–1952; f) I. Omae, *Coord. Chem. Rev.* **2004**, *248*, 995–1023; g) A. G. Fallis, *Acc. Chem. Res.* **1999**, *32*, 464–474; h) J. A. Marshall, *Chemtracts: Org. Chem.* **1992**, *5*, 111; i) S. C. Hirst, A. D. Hamilton, J. Rebek Jr, *Chemtracts: Org. Chem.* **1991**, *4*, 146; j) W. R. Roush, *Advances in Cycloaddition* (Ed.: D. P. Curran), JAI Press, Greenwich, CT, **1990**, vol. 2, pp. 91–146; k) M. E. Jung, *Synlett* **1990**, 186–190; l) D. Craig, *Chem. Soc. Rev.* **1987**, *16*, 187–238; m) E. Ciganek, *Org. React.* **1984**, *32*, 1; n) G. Brieger, J. N. Bennett, *Chem. Rev.* **1980**, *80*, 63–97; o) D. F. Taber, *Intramolecular Diels–Alder and Alder Ene Reactions*, Springer-Verlag, Berlin, **1984**; p) A. G. Fallis, *Can. J. Chem.* **1984**, *62*, 183–234; q) W. R. Roush, in *Comprehensive Organic Synthesis* (Eds: B. M. Trost, I. Fleming, L. A. Paquette), Pergamon, Oxford, **1991**, vol. 5, p. 513–550; r) D. Craig, "Stereoselective Synthesis" in *Methods of Organic Chemistry (Houben-Weyl)* (Eds: G. Helmchen, R. W. Hoffmann, J. Mulzer, E. Schaumann), 4th ed., Thieme, Stuttgart, **1995**, vol. E21c, pp. 2872–2904.

[2] Selected reviews on Type-2 IMDA: a) B. R. Bear, S. M. Sparks, K. J. Shea, *Angew. Chem. Int. Ed.* **2001**, *40*, 820–849; b) R. Keese, W. Luef, in *Topics in Stereochemistry* (Eds: E. L. Eliel, S. H. Wilen), Wiley, New York, **1991**, vol. 20, p. 231; c) P. M. Warner, *Chem. Rev.* **1989**, *89*, 1067–1093; d) W. T. Borden, *Chem. Rev.* **1989**, *89*, 1095–1109.

[3] Selected reviews: a) B. H. Lipshutz, *Chem. Rev.* **1986**, *86*, 795–819; b) B. A. Keay, I. R. Hunt, *Adv. Cycloaddition* **1999**, *6*, 173–210; c) C. O. Kappe, S. S. Murphree, A. Padwa, *Tetrahedron* **1997**, *53*, 14179–14233; d) L. M. Harwood, A. C. Brickwood, V. Morrison, J. Robertson, S. Swallow, *J. Heterocycl. Chem.* **1999**, *36*, 1391–1408; e) F. I. Zubkov, E. V. Nikitina, A. V. Varlamov, *Russ. Chem. Rev.* **2005**, *74*, 639–669.

[4] Selected recent articles on IMDAF: a) A. Padwa, H. Zhang, *J. Org. Chem.* **2007**, *72*, 2570–2582; b) H.-J. Wu, C.-F. Liu, Z. Wang, H.-C. Lin, *Tetrahedron Lett.* **2007**, *48*, 6192–6194; c) S. M. Sparks, C.-L. Chen, S. F. Martin, *Tetrahedron* **2007**, *63*, 8619–8635; d) M. Karaarslan, E. Gokturk, A. Demircan, *J. Chem. Res.* **2007**, 117–120; e) P. S. Sarang, A. A. Yadav, P. S. Patil, U. M. Krishna, G. K. Trivedi, M. M. Salunkhe, *Synthesis* **2007**, 1091–1095; f) M. E. Jung, S.-J. Min, *Tetrahedron* **2007**, *63*, 3682–3701; g) V. V. Kouznetsov, U. M. Cruz, F. I. Zubkov, E. V. Nikitina, *Synthesis* **2007**, 375–384; h) R. Pedrosa, S. Sayalero, M. Vicente, B. Casado, *J. Org. Chem.* **2005**, *70*, 7273–7278; i) H. Bruyere, C. Dos Reis, S. Samaritani, S. Ballereau, J. Royer, *Synthesis* **2006**, 1673–1681; j) S. K. Maurya, S. Hotha, *Tetrahedron Lett.* **2006**, *47*, 3307–3310; k) A. D. Mance, K. Jakopcic, *Mol. Diversity* **2005**, *9*, 229–231; l) K. M. Muller, B. A. Keay, *Synlett* **2008**, 1236–1238; m) E. S. Krygowski, K. Murphy-Benenato, M. D. Shair, *Angew. Chem. Int. Ed.* **2008**, *47*, 1680–1684.

[5] a) T. N. Cayzer, L. S.-M. Wong, P. Turner, M. N. Paddon-Row, M. S. Sherburn, *Chem. Eur. J.* **2002**, *8*, 739–750; b) D. J. Tantillo, K. N. Houk, M. E. Jung, *J. Org. Chem.* **2001**, *66*, 1938–1940; c) M. K. Diederich, F.-G. Klarner, B. R. Beno, K. N. Houk, H. Senderowitz, W. C. Still, *J. Am. Chem. Soc.* **1997**, *119*, 10255–10259; d) F. K. Brown, U. C. Singh, P. A. Kollman, L. Raimondi, K. N. Houk, C. W. Bock, *J. Org. Chem.* **1992**, *57*, 4862–4869; e) L. Raimondi, F. K. Brown, J. Gonzalez, K. N. Houk, *J. Am. Chem. Soc.* **1992**, *114*, 4796–4804; f) F. K. Brown, K. N. Houk, *Tetrahedron Lett.* **1985**, *26*, 2297–2300; g) O. Arjona, R. Medel, J. Plumet, R. Herrera, H. A. Jimenez-Vazquez, J. Tamariz, *J. Org. Chem.* **2004**, *69*, 2348–2354; h) L. R. Domingo, J. F. Sanz-Cervera, R. M. Williams, M. T. Picher, J. A. Marco, *J. Org. Chem.* **1997**, *62*, 1662–1667; i) J. Limanto, J. A. Tallarico, J. R. Porter, K. S. Khuong, K. N. Houk, M. L. Snapper, *J. Am. Chem. Soc.* **2002**, *124*, 14748–14758; j) L. R. Domingo, R. J. Zaragoza, R. M. Williams, *J. Org. Chem.* **2003**, *68*, 2895–2902; k) M.-D. Su, *Organometallics* **2004**, *23*, 2507–2509; l) K. S. Khuong, C. M. Beaudry, D. Trauner, K. N. Houk, *J. Am. Chem. Soc.* **2005**, *127*, 3688–3689; m) T. N. Cayzer, M. N. Paddon-Row, D. Moran, A. D. Payne, M. S. Sherburn, P. Turner, *J. Org. Chem.* **2005**, *70*, 5561–5570; n) M. N. Paddon-Row, D. Moran, G. A. Jones, M. S. Sherburn, *J. Org. Chem.* **2005**, *70*, 10841–10853; o) A. Padwa, K. R. Crawford, C. S. Straub, S. N. Pieniazek, K. N. Houk, *J. Org. Chem.* **2006**, *71*, 5432–5439; p) E. L. Pearson, L. C. H. Kwan, C. I. Turner, G. A. Jones, A. C. Willis, M. N. Paddon-Row, M. S. Sherburn, *J. Org. Chem.* **2006**, *71*, 6099–6109; q) H. Rabaa, B. Engels, T. Hupp, A. Stephen, K. Hashmi, *Int. J. Quantum Chem.* **2007**, *107*, 359–365.

[6] C.-C. Liao, C.-S. Chu, T.-H. Lee, P. D. Rao, S. Ko, L.-D. Song, H.-C. Shiao, *J. Org. Chem.* **1999**, *64*, 4102–4110.
[7] L. R. Domingo, M. J. Aurell, M. Arnó, J. A. Sáez, *J. Org. Chem.* **2007**, *72*, 4220–4227.
[8] I. N. N. Namboothiri, M. Ganesh, S. M. Mobin, M. Cojocaru, *J. Org. Chem.* **2005**, *70*, 2235–2243.
[9] **1a**: a) J. M. Chong, L. Shen, N. J. Taylor, *J. Am. Chem. Soc.* **2000**, *122*, 1822–1823; **1b**: b) S. Rajagopalan, P. V. A. Raman, *Org. Synth., Coll. Vol.* **1955**, *3*, 425; **1c**: c) C. F. H. Allen, F. W. Spangler, *Org. Synth., Coll. Vol.* **1955**, *3*, 377.
[10] R. Antonioletti, P. Bovicelli, S. Malancona, *Tetrahedron* **2002**, *58*, 589–596.
[11] a) L. Sader-Bakaouni, O. Charton, N. Kunesch, F. Tillequin, *Tetrahedron* **1998**, *54*, 1773–1782; b) T. Heiner, S. I. Kozhushkov, M. Noltemeyer, T. Haumann, R. Boese, A. de Meijere, *Tetrahedron* **1996**, *52*, 12185–12196; c) S. Woo, B. A. Keay, *Tetrahedron: Asymmetry* **1994**, *5*, 1411–1414.
[12] a) *JAGUAR*, ed. 5.5, Schrodinger Inc., Portland, OR, **2004**; b) W. J. Hehre, L. Radom, P. v. R. Schleyer, J. A. Pople, *Ab initio Molecular Orbital Theory*, Wiley-Interscience, New York, **1986**.
[13] a) A. D. Becke, *J. Chem. Phys.* **1993**, *98*, 5648–5652; b) C. Lee, W. Yang, R. G. Parr, *Phys. Rev. B* **1988**, *37*, 785–789.
[14] a) For a recent prediction of the regio- and steroselectivities in Diels–Alder reactions based on RHF/3-21G* results, see ref.[5g]; b) G. O. Jones, V. A. Guner, K. N. Houk, *J. Phys. Chem. A* **2006**, *110*, 1216–1224.
[15] A. Padwa, J. D. Ginn, S. K. Bur, C. K. Eidell, S. M. Lynch, *J. Org. Chem.* **2002**, *67*, 3412–3424.
[16] For a recent example of stereoselectivity control by torsional steering in an IMDA reaction, see: R. G. Iafe, K. N. Houk, *Org. Lett.* **2006**, *8*, 3469–3472.

Received: July 9, 2008
Published Online: November 18, 2008

